The Appalachian area as a tectonostratigraphic analogue for the Barents Sea shelf

Gustavo De Aguiar Martins[1], Frank Robert Ettensohn[1] and Stig-Morten Knutsen[2,3]

[1] Department of Earth & Environmental Sciences, University of Kentucky, Lexington, United States of America

[2]Norwegian Petroleum Directorate, Harstad, Norway

[3]Research Centre for Arctic Petroleum Exploration, UiT – The Arctic University of Norway, Tromsø, Norway

Correspondence

Gustavo De Aguiar Martins, University of Kentucky, 101 Slone Building, Lexington, Kentucky, United States of America.

Email: Gustavo.Martins@uky.edu

ACKNOWLEDGEMENTS

We wish to thank the Norwegian Petroleum Directorate (NPD) for providing the necessary funding for this research. We also acknowledge Alice Turkington and Aleksey Amantov for their constructive contributions and thank J. Richard Bowersox, Craig Magee, and an anonymous reviewer for their feedback, which greatly improved this text.

Abstract

The US Appalachian Basin and the Arctic Norwegian and Russian Barents Sea shelf (BSS) areas are two strategic provinces for the energy industry. The Appalachian Basin is a well-studied, mature, onshore basin, whereas the offshore BSS is still considered a frontier area. This study suggests that the Appalachian Basin may be an appropriate analogue for understanding the BSS and contribute to development of a tectonostratigraphic framework for the area. Although the Appalachian and BSS areas reflect different times and settings, both areas began as passive margins that were subsequently subjected to subduction and continent collision associated with the closure of an adjacent ocean basin. As a result, both areas exhibited multi-phase subduction-type orogenies, a rising hinterland that sourced sediments, and a foreland-basin sedimentary system that periodically overflowed onto an adjacent intracratonic area of basins and platforms with underlying basement structures. Foreland-basin sedimentary systems in the Mid-to-Late Paleozoic Appalachian Basin are composed of unconformity-bound cycles, related to specific orogenic pulses called tectophases. Each tectophase gave rise to a distinct sequence of lithologies related to flexural events in the orogen. In this study, similar sequences are recognized in both BSS foreland-basin and adjacent intracratonic sedimentary sequences that formed in response to the Late Paleozoic–Mesozoic Uralian-Pai-Khoi-Novaya Zemlya Orogeny, suggesting that the processes generating the sequences are analogous to the tectophase cycles in the Appalachian Basin. Hence, this pioneering use of the Appalachian area and its succession as large-scale tectonostratigraphic analogues for the BSS may further enhance understanding of Upper Paleozoic to Middle Jurassic stratigraphy across the BSS.

KEYWORDS

Appalachian orogenies, Uralian Orogeny, tectophases, petroleum basins, foreland basins, intracratonic basins, basement precursor structures

1 INTRODUCTION

The use of analogues is recognized as an important tool in providing solutions for qualitative and quantitative problems pertinent to both academia and the energy industry (e.g., Howell et al., 2014; Schellart and Strak, 2016; Sun et al., 2021). Analogues are especially desirable when dealing with areas where geological uncertainties predominate. Use of geological analogues typically involves using a well-known geological system, area, or process (the standard) to help explain possible similarities between the standard and a target of interest. For example, Ulmishek (1986) suggested that the assessment of undiscovered hydrocarbon resources in poorly known areas (targets of interest) should be based on comparative analysis of geologic elements and processes in a well-explored analogue area (standard). In this study, the well-known geological evolution of the onshore, east central, US Appalachian region (Fig. 1A), including the foreland basin and adjacent cratonic area, is the standard, whereas the Barents Sea shelf (BSS) (Fig. 1B) is the target area of interest. The BSS is part of the Norwegian (western BSS) and Russian (eastern BSS) Arctic continental shelf and currently represents a frontier province—in particular the northern sectors—for hydrocarbon exploration, and for future carbon storage capture (NPD, 2017).

The BSS is commonly characterized as a large tectonic element within the Arctic system of platforms and basins (e.g., Drachev, 2016). Even though the BSS is a well-studied Arctic region, research focusing on external, large-scale, tectonostratigraphic analogues to the overall setting and development of the BSS remains scarce. Hence, the overarching goal of this paper is

to investigate possible analogue relationships between the U.S. Appalachian and BSS systems of basins and platforms. Elements of the Appalachian system (Fig. 1A) have been previously used as possible analogues for the nearby Timan-Pechora Basin (e.g., Artyushkov and Baer, 1986), and earlier generic comparisons of the Appalachian orogen with the Caledonian and Uralian orogens have been attempted (Arthaud and Matte, 1977; Artyushkov and Baer, 1983, 1985; Kruse and McNutt, 1988; Knapp et al., 1998; Matte, 2002; Brown et al., 2004, 2006b; Puchkov, 2009; Hatcher, 2010; Allen and Allen, 2013). For example, Puchkov (2009) briefly suggested that evolution of the Uralian Orogeny was like that of the Taconian and Alleghanian orogenies in the Appalachian area but went no further in defining the analogue. Difficulties in developing suitable regional external analogues for the offshore BSS probably result from lack of familiarity with possible analogue basins and the fact that the BSS is not as well explored as other regions. In fact, Scott (2007) published a report entitled, “Eastern Barents Sea-Novaya Zemlya-Kara Sea tectonic relationships: The search for an appropriate analogue,” which highlights the importance of finding suitable analogues for the BSS.

Accessibility to BSS data can also be difficult. In the Norwegian sector, data from several exploration-wells and seismic surveys are available also through the Norwegian Petroleum Directorate (NPD). However, wells concentrate in southwestern-most areas and a large majority did not reach Paleozoic strata. Moreover, the northern sector (>74°30’N) has not yet been opened for petroleum activity (NPD, 2017), and seismic quality is often poor, and most is only two-dimensional. In the Russian sector, data tend to concentrate in southern areas and are very difficult to obtain except what is published. Unlike the Norwegian Svalbard archipelago (Fig. 1), access to the Russian Novaya Zemlya archipelago is restricted. Clearly, the above situation makes it challenging to generate large-scale studies capable of integrating both sectors of the

BSS. As a result, BSS problems, such as far-field tectonics, halokinesis, energy potential, stratigraphic facies, regional tectonism, among others, remain more unresolved to the north. In trying to resolve these issues, several analogues have been used at various scales, but with varying degrees of success. What has been lacking, however, is a large-scale, analogue-generated model to integrate all these aspects across the BSS. Hence, in this study we present the Appalachian foreland basin and adjacent intracratonic areas as such a large-scale analogue capable of treating all these aspects together, thus, representing another instrument in the BSS analogue toolbox.

The geology and tectonostratigraphy of both Appalachian and BSS areas are largely the result of their development within the classic framework of the Wilson cycle (Wilson, 1966; Puchkov, 2009; Ettensohn et al., 2019), which necessarily includes such large-scale tectonic elements as passive margins, foreland basins and intracratonic platforms (e.g., Walcott, 1970; Price, 1973; Beaumont, 1981). The Appalachian foreland basin and adjacent intracratonic platforms and basins are considered sources of potential analogues for comparison, because they represent the “type-area” of the Wilson cycle (Wilson, 1966; Ettensohn et al., 2019) and also the “type-area” for related tectonostratigraphic sequences (Hatcher et al., 1989; Tollo et al., 2010). Consequently, the Wilson cycle and the resulting tectonostratigraphic sequences provide the foundation for testing this hypothesis of basin analogues.

Hence, the overarching goal of this paper is to define and test the above analogue hypothesis by providing a review of the main tectonostratigraphic features of the BSS and systematically comparing them with those of the Appalachian foreland basin and adjacent intracratonic areas. Because no seismic data were available for this study, our interpretations are based largely on published literature.

1.1 ANALOGUE POTENTIAL AND TESTING

Geologic studies frequently rely on analogues because the development of rocks and structures can rarely be observed directly (Alexander, 1993). This is true for the BSS because: 1) the area is mostly submerged; 2) seismic imaging to the north is often poor; 3) well data north of 74°30'N are often limited or non-existent; 4) most wells do not hit basement; 5) Russian data are mostly inaccessible; 6) structural elements are widespread and frequently affected sedimentation; and 7) several orogenic events affected the area and overlapped in time and space (see section 2). Hence, choosing analogues applicable at both local and regional scales and capable of integrating both shelf sectors is difficult. For example, an analogue employed to understand the Nordkapp Basin, a rift basin (Fig. 1), may fail in explaining the South Barents foreland basin. To help with addressing such challenges, after examining several basinal areas, we chose the following key aspects of the Appalachian area for comparison with the target BSS area: 1) areal extent; 2) evidence for multiple tectonic events of similar types and durations; 3) presence of coeval, far-field, structural reactivation; and 4) presence of foreland-basin and an adjacent intracratonic areas with distinctive tectonostratigraphic sequences. Testing for each of these aspects required a systematic comparison of the standard (Appalachian area) with the target (BSS) (see Table 1).

Relative to areal extent, although not equal, the extent of the Appalachian area (0.93 million km^2) approaches that of the BSS (1.4 million km^2). Furthermore, in both areas, tectonic events largely tie to key Pangean Wilson cycles. In the Appalachian area, the cycle involved opening and closure of the Iapetus and Rheic oceans, whereas in the BSS area the cycle involved opening and closure of the Iapetus and Uralian oceans, both of which triggered multiple, diachronous, continent-margin orogenies (e.g., Ziegler, 1989; Matte, 2002; Puchkov, 2009;

Hatcher, 2010). In fact, Puchkov (2009) noted that the duration of the Uralian Orogeny (~214 Ma; Middle Devonian–Middle Jurassic; eastern BSS) is comparable to that of the Appalachian orogenies (~217; Middle Ordovician–Permian; Appalachian area). Moreover, in both areas, subduction-type orogenies preceded final continent-continent collision. Importantly, these orogenies also reactivated widespread basement structures, which, on the BSS, are largely Precambrian to Caledonian in age (Anell et al., 2013), and in the Appalachian area, are Precambrian to Cambrian in age (Ettensohn et al., 2019). Similarly, these tectonic events resulted in distinctive, geometrically comparable, tectonostratigraphic successions of carbonates and clastics that can be characterized in similar terms in both areas (cf., NPD, 2017; Ettensohn et al., 2019; see Section 2). Nonetheless, challenges related to different paleogeography, paleoclimate, and timing remain. However, these challenges do not necessarily invalidate the basic tectonic mechanisms that underpin the analogous development of both areas.

Although the tectonic development and stratigraphic framework of the Appalachian area are already well-known (e.g., Ettensohn et al., 2019), these same aspects of the BSS, especially for the eastern Russian sector, are incompletely known. Our first step, then, in testing analogies was to understand the regional stratigraphy of the BSS. This was accomplished through an extensive review of the literature and NPD archives, which resulted in a stratigraphic chart/section that encompasses most of the BSS (see Section 2). Searching this chart/section for cyclic, unconformity-bound, stratigraphic responses, comparable with those in the Appalachian area represented a critical test of the analogue, because presence of such cycles is evidence of similar tectonic mechanisms, which were already developed for the Appalachian area (see Section 3). In the end, application of Appalachian tectonostratigraphy as an analogue allowed the

interpretation of the late Paleozoic to Middle Jurassic BSS succession in term of flexural tectonics.

2 GEOLOGICAL SETTING

2.1 Barents Sea shelf (BSS)

The BSS covers approximately 1.4 million km^2 and comprises the sea-areas with average water-depths of about 230 m located between northern Norway, Svalbard, Franz Joseph Land, and Novaya Zemlya (Fig. 1B). The regional structural framework includes large basins west of Novaya Zemlya, which gently pass westward into an extensive platform area with smaller basins (Marello et al., 2013) (Fig. 1B). The very southeastern end of the BSS is defined as the Timan-Pechora Basin, which continues onshore areas (Stephenson et al., 2006; Stoupakova et al., 2011). The eastern and western areas of the BSS are delimited by an overall N-S monoclinal structure that roughly corresponds with the offshore boundary between the Norwegian and Russian sectors (Worsley, 2008; Faleide et al., 2017) (Fig. 1B). The geologic evolution of the eastern BSS was mainly influenced by the Uralian Orogeny (e.g., Petrov et al., 2008), whereas the western BSS had multiple influences, including Caledonian and Uralian orogenic events, followed by the late Mesozoic–Paleogene opening of the North Atlantic (e.g., Worsley, 2008).

The eastern BSS sector consists of two very deep basins (Fig. 1B), with thicknesses of possibly more than 20 km in the South Barents Basin and 12 km in the North Barents Basin (Gee, 2005; Ivanova et al., 2006; Shipilov, 2010; Klitzke et al., 2015), which cover a basement of most likely Timanian (Late Proterozoic–Early Cambrian) origin (Gee et al., 2006; Kuznetsov, 2006; Drachev, 2016). Timanian basement structures trend NW-SE and are truncated by Uralian and Caledonian structures, on the eastern and western margins of the BSS, respectively (Pease et

al., 2014; Gernigon et al., 2018). The western BSS sector exhibits many smaller basins and intervening platforms, with sedimentary thicknesses of at least 10 km (Faleide et al., 1984). These western basins have a basement of likely Caledonian origin (Gee et al., 2010; Corfu et al., 2014; Klitzke et al., 2019), originating from the Silurian–Devonian continental collision of Baltica and Laurentia that formed the supercontinent Laurussia (Ziegler, 1989; McKerrow et al., 2000; Torsvik and Cocks, 2017; Miall and Blakey, 2019). The dominant Caledonian structural trends are N-S and NE-SW (Gee et al., 2008; Gernigon et al., 2014) (Fig.1B).

In general, the tectonostratigraphic framework of the BSS is represented by a clastic-carbonate-clastic succession (Figs. 2, 3) that reflects complex relationships among tectonics, eustasy, paleogeography, and paleoclimate. Ordovician to Middle Devonian rocks have only been identified in the eastern BSS basins and include organic-rich rocks that sourced large volumes of hydrocarbons (Alsgaard, 1993; Guo et al., 2010; He et al., 2012; Polyakova, 2015; Stoupakova et al., 2011, 2015). During Early Devonian to Early Carboniferous time, the BSS migrated out of equatorial and into subtropical conditions (Worsley, 2008; Lopes et al., 2016). Continental and marginal-marine clastics were deposited in western parts of the shelf (Figs. 2, 3, B’-B’’), while widespread carbonate sedimentation predominated in shallow-marine basins across the eastern parts of the shelf (Stemmerik and Worsley, 2005; Dallmann et al., 2015) (Fig. 3, C-C’, B-B’). Ongoing sea-level rise, regional uplift and development of half-grabens favored deposition of thick warm-water carbonate successions, including buildups and lagoonal evaporites on the BSS during Carboniferous and Early Permian time. (Stemmerik et al., 1994; Stemmerik and Worsley, 2005; Rafaelsen et al., 2008; Blomeier et al., 2009) (Figs. 2, 3). In the eastern BSS during Late Carboniferous–Early Permian time, black, phosphate-bearing, siliceous, radiolarian-rich, shales grade eastward into turbidite deposits (Smelror et al., 2009) (Figs. 2, 3).

On the western BSS, Upper Carboniferous to Lower Permian deposits include algal build-ups and limestones locally intercalated with evaporites (Dallmann et al., 2015). By Early Mid Permian time, the BSS had migrated into more temperate latitudes, contributing to the shift in regional deposition from shallow, warm-water to deeper-water carbonates and spiculitic cherts (Stemmerik, 2000; Matysik et al., 2018) (Figs. 2, 3). Moreover, Upper Permian petroleum source-prone, calcareous, silica-rich, black shales have been identified in both the Norwegian and Russian Barents Sea shelves (Figs. 2, 3), having thicknesses of ~100 m and ~350 m respectively (Henriksen et al., 2011; Konyukhov, 2016). During Late Permian–Early Triassic time, the Uralian Orogeny culminated, resulting in rapid crustal subsidence and deposition of flysch- and molasse-like sediments in the eastern BSS (Faleide et al., 1984; Nikishin et al., 1996; Golonka and Ford, 2000) (Fig. 3). As the Uralides evolved, large volumes of clastics, initially consisting of prolific organic-rich muds (Figs. 2, 3), were deposited across the BSS (Johansen et al., 1993; Brekke et al., 1999; Riis et al., 2008; Anell et al., 2014, 2016; Lundschien et al., 2014; Konyukhov, 2016; Uchman et al., 2016). During Mid Triassic–Early Jurassic time, uplifted Uralian source areas to the east contributed large volumes of prograding clastic sediments, whereas on parts of the western shelf, deposition of source-prone black shales predominated (Ohm et al., 2008; Stupakova et al., 2012; Polyakova, 2015; Georgiev et al., 2017) (Figs. 2, 3). During Late Jurassic to earliest Cretaceous time, Kimmeridgian rifting and deposition of organic-rich black shales marked the inception of North Atlantic tectonism across the BSS (Figs. 2, 3) (Lopatin, 2003; Faleide et al., 2008; Henriksen et al., 2011; Serck et al., 2017). Events associated with the opening of the North Atlantic Ocean may have started as early as Late Paleozoic–earliest Triassic and persisted into Cenozoic time (Knutsen and Larsen, 1997; Ryseth et al., 2003; Stemmerik and Worsley, 2005; Amantov and Fjeldskaar, 2018).

2.2 Uralian-Pai-Khoi-Novaya Zemlya Orogeny

The traditionally named “Uralian-Pai-Khoi-Novaya Zemlya” Orogeny (Volkov, 1963), was the product of the collision of Siberia and Kazakhstania with the Baltic margin of Laurussia (Puchkov, 1997, 2003; Brown et al., 2004; Pease et al., 2014; Torsvik and Cocks, 2017). The Uralide belt is today represented by a N-S linear belt, at least 2500 km in length (Fig. 4A), which represents the Paleozoic collision of at least two intra-oceanic arcs at the eastern margin of Baltica, followed by continent-continent collision (Brown et al., 2006a; Puchkov, 2009).

Broadly viewed, the orogeny developed in Paleozoic (Ordovician–Permian) and Mesozoic (Triassic–Jurassic) stages (Puchkov and Ivanov, 2020). The Paleozoic stage in the BSS area is tied to the closure of the Uralian Ocean during Early Carboniferous to Permian time, with the main orogenic phase taking place in Late Permian to Early Triassic time (Ershova et al., 2015; Petrov et al., 2016; Smelror and Petrov, 2018). The foreland basin for this stage of collision was concentrated in the present-day Novaya Zemlya area and was filled with dark shales, flysch-like and molasse-like sediments (Figs. 2, 3, 4) (Brown et al., 2006a, Reid et al., 2007; Puchkov, 2009).

The late stages (at least Late Mesozoic) of the Uralian Orogeny are often called the Pai-Khoi-Novaya Zemlya Orogeny (Smelror and Petrov, 2018; Puchkov and Ivanov, 2020). Pai-Khoi (Figs. 1B, 4) is a complex structural area between what is now the Novaya Zemlya archipelago and the northernmost Ural Mountains (Timonin et al., 2004). Novaya Zemlya (Figs. 1B, 4) is an arc-shaped archipelago, which has been interpreted as the result of the Late Triassic to Early Jurassic collision of Siberia, which acted as a transpressional indenter, with a former continental embayment on the northeastern margin of Baltica (Lopatin et al., 2001; Petrov et al.,

2008; Smelror et al., 2009; Scott et al., 2010; Faleide et al., 2017; Curtis et al., 2018; Smelror and Petrov, 2018; Puchkov and Ivanov, 2020). During this phase of orogeny, what had been a Late Paleozoic foreland basin became inverted as a fold-thrust belt and pushed westward onto the margin of Baltica as the current, arc-shaped Novaya Zemlya archipelago. Puchkov (2009) interpreted this Mesozoic phase to represent the terminal collision in the Uralides. The resultant Novaya Zemlya fold belt (archipelago) is approximately 1200 km in length (Fig. 4A), represents the amalgamation of several allochthons, and exposes Precambrian to Early Triassic successions (Filatova and Khain, 2010; Toro et al., 2016; Zhang et al., 2018). The geographic position of the archipelago suggests that it represents a northward continuation of the Uralian Orogeny, but such a possibility is still debated (Dedeev, 1959; Volkov, 1963; Otto and Bailey, 1995; O'Leary et al., 2004; Buiter and Torsvik, 2007; Scott et al., 2010; Pease et al., 2014; Toro et al., 2016; Smelror and Petrov, 2018). Although a major tectonic analysis of Novaya Zemlya is beyond the scope of this paper, it is important to be aware that the development of the Novaya Zemlya fold belt significantly influenced the tectonostratigraphy on the BSS.

2.3 Appalachian Basin

The Appalachian Basin represents a large-scale, composite foreland basin associated with the amalgamation of Pangea (e.g., Hatcher et al., 1989). The Appalachian Basin is approximately 2050 km in length and is about 530 km at its broadest point and includes an area of approximately 536,000 km^2 (Colton, 1970). The stratigraphic succession is wholly Paleozoic, with thicknesses of nearly 600 to 900 m on its western flank and more than 13,700 km on its eastern flank, and a total sedimentary volume of about 2,300,000 km^3 (Ettensohn et al., 2019). Large intracratonic basins occur to the west (Fig. 1A), and to the east, the Appalachian Mountain

belt has a NE-SW orientation and a length of 3000 km (Hatcher, 2010). Moreover, some workers include the Ouachita fold belt (Fig. 4B) as a structural extension of the Appalachian system that extends southwestward for an additional 2100 km (Thomas, 1985; Denison, 1989; Viele, 1989; Miall and Blakey, 2019). In a broad view, the Appalachian Basin and adjacent intracratonic areas reflect subsidence accompanying a series of terrane collisions with the Appalachian margin during at least five orogenies (Ettensohn et al., 2019). These tectonic events contributed to the development of Pangea and represent one complete Wilson cycle (Stockmal et al., 1998; Hatcher, 2010; Miall and Blakey, 2019).

The tectonostratigraphic framework of U.S. parts of the Appalachian Basin is represented by a clastic-carbonate-clastic succession (Fig. 5), which reflects complex relationships among tectonics, eustasy, paleogeography, and paleoclimate. The succession began with the deposition of continental clastics in rift basins formed during the initiation of the Iapetan cycle during Late Precambrian–Early Cambrian time (Curtis and Faure, 1997; Gao et al., 2000). Laurentia shifted southward from its Late Precambrian equatorial position, and by Cambro–Ordovician time, the Appalachian margin had reached subtropical, arid latitudes, contributing to thick carbonate successions along the passive margin (Torsvik and Cocks, 2017; Miall and Blakey, 2019) (Fig. 5). By the Early–Middle Ordovician transition, island-arc collision with promontories on the Appalachian margin generated the Taconian Orogeny and a concomitant regional unconformity across large parts of Laurentia (Sloss, 1963; Finney et al., 1996; Park et al., 2010) (Fig. 5). At the time, the Appalachian region remained within arid latitudes (Torsvik and Cocks, 2017) and produced a foreland-basin succession including black-shale deposition of excellent petroleum potential within and beyond the foreland basin (Park et al., 2010; Ettensohn et al., 2019). The Appalachian margin remained in arid latitudes until Late Mississippian time, and during this

period, experienced a series of orogenic events, the Salinic and Acadian/Neoacadian orogenies (Hatcher, 2010; Ettensohn et al., 2019; Miall and Blakey, 2019). These orogenic events generated foreland-basin deposits that include widespread black-shales, as well as coarser-clastic and carbonate sequences that comprise one of the most prolific petroleum systems within the foreland and adjacent intracratonic basins (Cluff and Dickerson, 1982; Roen, 1984; Ettensohn, 1985; Ettensohn and Lierman, 2012; Konyukhov, 2014) (Figs. 1A, 5). By Late Mississippian–Early Pennsylvanian time, the Appalachian margin moved into the tropical, equatorial belt (Torsvik and Cocks, 2017). At the same time, continent-continent collision with Gondwana generated the Alleghanian Orogeny (Hercynian-Variscan), and a fold-thrust belt that filled the adjacent foreland basin with a coal-rich clastic blanket that prograded more than 1000 km westward across the craton (Hatcher et al., 1989; Greb et al., 2008; Ettensohn et al., 2019) (Fig. 5). By Late Triassic–Jurassic time, global plate-tectonic reconfiguration led to widespread rifting along the former Appalachian Mountain belt, initiating the Atlantic Wilson cycle (Miall and Blakey, 2019).

3 APPALACHIAN AND BSS ANALOGUES

3.1 Large-scale tectonic analogues

It is very true that perfect analogues do not exist (Alexander, 1993), but on a broad scale, as imperfect as they are, as comparisons, analogues can still prove to be very useful. Howell et al. (2014) have noted that at the largest scales, analogues of size and geometry of geological features may be effective ways to begin the comparison of two areas, and such a comparison can be done between the Appalachian and BSS regions (Table 1). Both areas contain basins filled with thick sedimentary successions and include regions exhibiting foreland and hinterland

physiographic domains. Both hinterlands exhibit multi-generational mountain belts that formed through diachronous subduction/collisional events associated with ocean closure. In the Appalachian region, the Iapetus and Rheic oceans closed during several Paleozoic collisions with peri-Gondwanan microcontinents and Gondwana (e.g., Hatcher et al., 2007). Closure of the Iapetus Ocean continued northward into the western BSS region with collision of Baltica and Laurentia to form the minor supercontinent Laurussia and the Arctic-North Atlantic Caledonides (e.g., Corfu et al., 2014).

Although the BSS is about one-third larger than the Appalachian region, both areas exhibit similar large-scale tectonic features (Fig. 1; Table 1). For the Paleozoic, Appalachian hinterland (now mostly eroded), the analogous BSS feature is the Late Paleozoic–Mesozoic Uralian and Novaya Zemlya hinterland, suggested by Puchkov (2002) to be structurally analogous features. Cratonward (west) of the Appalachian hinterland is the Appalachian foreland basin, which was superimposed on Late Precambrian precursor rift basins (Rome Trough, Fig. 1A; Ettensohn, 2008). Similarly, cratonward of the Uralian hinterland is an extensive foreland-basin belt extending from the Caspian Sea to Novaya Zemlya (Fig. 4C), including Novaya Zemlya itself in Late Paleozoic time and later incorporating the South and North Barents basinal areas in Permo-Triassic time and again in Late Triassic–Jurassic time (Nikishin et al., 2002; Müller et al., 2019). The Uralian succession across the BSS was similarly superimposed on Caledonian and Timanian basement structures.

Cratonward of the Appalachian Basin is a transitional area, represented by the Cincinnati Arch (Fig. 1A), interpreted to have been a Pennsylvanian–Permian, Alleghanian bulge (Tankard, 1986), which resembles the broad monoclinal structure between the western and eastern BSS sectors interpreted here to be a transitional bulge-like zone. Others have interpreted even larger

areas of the western BSS to have been a Jurassic, Uralian-Pai-Khoi-Novaya Zemlya bulge (e.g., Müller et al., 2019) (Fig. 6). West of the Alleghanian bulge area in the Appalachian region, is a broad, foreland zone of large intracratonic basins and intervening platform areas, most of which probably began as reactivated rift basins (Klein and Hsui, 1987). This broad intracratonic region is rife with older basement structures (Fig. 1A), which were periodically reactivated by far-field tectonics during the various Appalachian orogenies (Ettensohn et al., 2019). In the Norwegian BSS, a broad platform system, basins and uplifts are similarly underlain by Caledonian, basement structures, which may have been reactivated by far-field tectonics during the Uralian Orogeny (Anell et al., 2013).

Like tectonics, the paleoclimatic evolution in both areas is comparable because the succession of paleoclimates represents a shift from humid to arid, and again to humid conditions (Table 1). It is important to note that even though the succession of paleoclimates in both areas was similar, the paleogeographic position was not. In a broad view, the humid conditions in the Appalachian area were due to its more equatorial position, whereas the BSS was influenced by both equatorial and highly temperate zones as the area moved to its current geographic location (Miall et al., 2019). Such tectonic and paleoclimate similarities led to the development of largely comparable stratigraphic successions, which include multiple regional unconformities and the persistence of carbonate platforms (Figs. 2, 3, 5; Table 1).

3.2 Tectonic process analogues

The similarities between Appalachian and BSS regions reflect largely comparable tectonic histories. The Paleozoic development of the Appalachian region reflects the closure of seaway and continent-continent collision (Hatcher, 2010). After development of a Cambro-

Ordovician, carbonate-rich, passive margin, a mid-Ordovician to Mississippian phase involving the westward, subduction-related collision of island arcs and peri-Gondwanan terranes, generated several marine, facies-rich foreland basins, which migrated westward in space and time (Ettensohn, 2008). During the four orogenies involved, the accompanying foreland basins developed cyclic, unconformity-bound, sedimentary sequences in response to the orogeny; these sedimentary sequences have been termed tectophase cycles by Johnson (1971) and Ettensohn et al. (2019). Far-field forces during subduction promulgated the reactivation of extensive basement rift systems across the adjacent foreland. This phase ended with continent-continent collision and the generation of an extensive, Pennsylvanian–Permian clastic wedge (Fig. 5). Subsequent Late Triassic–Jurassic rifting and sedimentation ended the Appalachian Wilson cycle and marked the inception of the Atlantic cycle (Ettensohn et al., 2019). The evolution of the Appalachian area can be condensed into eight stages, which are summarized in Table 2.

If the Appalachian evolution (Table 2) is seen as a large-scale analogue to the BSS area, then similar evolutionary stages should be observed in both areas. Although the Arctic-North Atlantic Caledonides generated the basement in western parts of the BSS and many of the structures therein, we will not include them in this comparative analysis, because the resulting sedimentary succession was largely eroded (Nikishin et al., 1996). Instead, we will use the well-preserved Late Paleozoic–Mesozoic Uralian-Pai-Khoi-Novaya Zemlya succession and structures on the BSS, because, as in the Appalachian area, they are the products of diachronous collisional events associated with the closure of the Uralian Ocean (Puchkov, 2009).

In the BSS, several basement structures were developed during the Timanian and Caledonian orogenies, and these were later reactivated by the collapse of the Caledonides, and during the Uralian-Pai-Khoi-Novaya Zemlya Orogeny (Anell et al., 2013). This event

corresponds to stages 1 and 2 in the Appalachian area (Table 2) where a regional framework of pre-Appalachian basement structures was reactivated by the multiple Appalachian orogenies (Ettensohn, 2008). In both areas, orogenic collapse triggered relaxation, rifting and erosion, and widespread deposition of mainly continental-clastic sequences (Figs. 2, 3, 5; Table 2). Next, in the BSS region, a Late Mississippian to Early Permian, carbonate-rich stable platform developed behind a Middle Devonian island arc above the westward subduction of the Uralian oceanic plate on the eastern BSS area (e.g., Ziegler, 1989; Smelror et al., 2009) (Figs. 2, 3). This event corresponds to stage 3 in the Appalachian area (Table 2), where a stable platform rich in carbonate rocks developed during the Middle Cambrian–Early Ordovician (Fig. 5).

By Pennsylvanian time, major subduction, involving arc collision on the eastern BSS region (Ziegler, 1989; Nikishin et al., 1996), is represented by a regional Late Carboniferous–Permian unconformity (Fig. 3), which marks the inception of crustal loading in the Novaya Zemlya/eastern BSS region. This event corresponds to stage 4 in the Appalachian area (Table 2), where crustal loading triggered by the Taconian Orogeny is represented by a regional Middle Ordovician unconformity (Fig. 5). The increasing crustal loading in the Novaya Zemlya/eastern BSS area eventually triggered widespread deformational loading, which is represented by the extensive deposition of cherty limestones to black shales (Fig. 3), representing basal foreland-basin sequences. This event corresponds to stage 5 in the Appalachian area (Table 2), where the inception of the Appalachian foreland basin (Ettensohn et al., 2019) is represented by the deposition of carbonates and black shales overlying the Middle Ordovician unconformity (Fig. 5). Following crustal loading, the Novaya Zemlya/eastern BSS area rebounded. Widespread flysch-like and molasse-like sequences were deposited in that area during Permian to Late Triassic time and are represented by black shales and marine to marginal-marine clastics (Fig. 3).

This event corresponds to stage 6 in the Appalachian area (Table 2), which was repeated during each Appalachian orogenic pulse and explains the deposition of multiple foreland successions (Ettensohn et al., 2019) (Fig. 5). In the BSS, at least two phases of crustal loading and relaxation are apparent during at least Late Triassic time (Fig. 3). Lastly, one final tectonic pulse thrusted Novaya Zemlya on top of the eastern BSS (Petrov et al., 2008), generating a regional Triassic–Jurassic unconformity and resulting in the deposition of Lower–Middle Jurassic marine, marginal-marine and terrestrial clastic sequences (Fig. 3); this represents the termination of the Uralian-Pai-Khoi-Novaya Zemlya cycle (Petrov et al., 2008; Henriksen et al., 2011). This event corresponds to stage 7 in the Appalachian area (Table 2), during which Pennsylvanian–Permian continental collision (Alleghanian Orogeny) triggered regional unconformity development and a subsequent, largely terrestrial, clastic wedge (Fig. 5), which represents the termination of the Appalachian cycle (Ettensohn et al., 2019). In the BSS area, Late Jurassic–Eocene rifting, associated with the opening of the North Atlantic Ocean and the polar basin to the far west and north, respectively, became the dominant tectonic process. These events correspond to stage 8 in the Appalachian area (Table 2), during which Late Triassic–Jurassic rifting is associated with the opening of the Atlantic Ocean.

3.3 Foreland-basin analogues

Foreland basins represent a flexural crustal response to an advancing deformational load, the erosion of which largely provides the infilling sediments (Quinlan and Beaumont, 1984). Such foreland crustal responses may propagate across distances of more than 1000 km (Beaumont, 1981; DeCelles and Giles, 1996) and reflect a dynamic relationship between tectonics and depositional regime (Figs. 7A, 7B). Deformational loading in the form of a fold

and thrust belt develops in response to orogeny, generating subsidence in front of the load, as a subsiding foreland basin and an uplifted peripheral bulge on the distal edge of the foreland basin. Uplift on the bulge typically generates an unconformity, and as the load migrates cratonward, the basin, bulge and contained sediments will also migrate cratonward (Fig. 7; Quinlan and Beaumont, 1984).

The tectonic setting of the Appalachian Basin has been used to construct tectonostratigraphic models for foreland-basin sedimentation (Johnson, 1971; Ettensohn, 1991, 2004, 2008; Ettensohn et al., 2019), and following similar lines of thought, Johnson (1971) used the concept of "tectophase cycles" to predict, discuss, and illustrate the tectonostratigraphic succession of a foreland basin. Inasmuch as subduction-related orogenies occur in a series of deformational pulses or "tectophases" (Johnson, 1971; Jamieson and Beaumont, 1988; Camacho et al., 2005), each tectophase will generate a typical sequence of lithologies (Fig. 8), representing isostatic responses to the changing deformational load. In collisional orogenies, however, lower parts of a typical cycle are wholly overwhelmed by widespread, thin-skinned uplift and accompanying terrestrial sedimentation, as in the Appalachian Alleghanian Orogeny. Several examples of tectophase sequences are present in the Appalachian Basin (Ettensohn et al., 2019), but the Mississippian sequence, a stratigraphic response to the Neoacadian Orogeny (Fig. 9), probably provides the best example of the model.

According to Ettensohn et al. (2019), a typical foreland-basin sequence (Fig. 8) begins with a regional unconformity marking bulge uplift and moveout (Figs. 8, 9A). In addition to these regional, sequence-bounding unconformities, more localized unconformities may also occur due to far-field reactivation of local basement structures. Bulge uplift and moveout is followed by initial subsidence typically represented by the rapid deposition of shallow-water

carbonates or sands (Fig. 8), but this phase may be absent where subsidence is very rapid (Fig. 9A). Once load migration ceases and the load becomes static, subsidence outpaces sedimentation, as most of the load is subaqueous and generates little clastic sediment (Fig. 7A). As a result, mostly fine-grained organic matter from the water column accumulates. Many foreland-basin source rocks originate in this fashion (Ulmishek and Klemme, 1990; Ettensohn, 1997).

As surficial relief and complete drainage nets develop, clastic sediments from the adjacent load fill the foreland basin with “flysch-like” sediments represented by deep- to shallow-marine, clastic deposits (Figs. 7B, 8, 9B). Once filled, the basin passes through a short “equilibrium” phase, during which basin fill and eroded source areas are at or near base level; distal parts of the basin may experience sediment starvation at this time (Fig. 9C). In the Mississippian example from the Appalachian Basin (Fig. 9), equilibrium carbonates predominate during this phase because of unique subtropical, lowstand conditions in the area (Fig. 9D). However, this phase may be minimal or absent in different climatic or non-lowstand conditions. The equilibrium phase is followed by a relaxation phase when proximal parts of the foreland basin and adjacent “unloaded” source areas (Fig. 9D) undergo rebound (Fig. 9E), and previously deposited sediments are cannibalized. This phase is dominated by widespread deposition of finer-grained, marginal-marine, post-orogenic, clastic sediments, which often include redbeds and coals. These “molasse-like” sediments (Fig. 8) end the tectophase cycle and are typically truncated by a regional unconformity marking the inception of the next tectophase. Tectonostratigraphic sequences like the tectophase cycle have been recognized in several other foreland basins (Allen et al., 1991; Sinclair et al., 1991; Coakley and Watts, 1991; Su et al., 2009).

However, each foreland basin is different in the number of cycles, each of which reflects an orogenic event. For example, the Alpine foreland basin exhibits only one cycle (Allen et al., 1991; Sinclair et al., 1991), whereas the Appalachian Basin exhibits 13 such cycles reflecting five orogenies, of which cycles beginning with the Ordovician Utica (Fig. 10) and Devonian Marcellus (Fig. 11A) black shales are best known for their hydrocarbon potential. Of special interest relative to foreland-basin cycles are the two Taconian tectophase cycles in the Appalachian Basin (Fig. 10). Figure 10 illustrates one ideal case of well-developed cycles in an along-strike section that shows how orogeny and accompanying cycles migrate in space and time (south to north), as well as the varying tectonostratigraphic responses in each of the two cycles. On the BSS, we have recognized three such tectophase successions (Fig. 3) reflecting two major orogenic events.

Using Appalachian Basin models (Figs. 8–11A) as a basis, a schematic cross section illustrating the tectonostratigraphic development of the Late Permian–Middle Jurassic succession across the BSS is presented (Fig. 11B). This model illustrates multiple tectonic pulses in the eastern BSS region and a largely southeastern to northwestern progradation of deeper-marine shales and clastic wedges. The formation names correspond to the Norwegian nomenclature currently adopted by the Norwegian Petroleum Directorate. At least three major clastic wedges were deposited during Late Permian, Triassic, Late Triassic (Norian) and Middle Jurassic times (Fig. 11B). To our knowledge, the only wedge with a “formal” name is the “Triassic Boreal Ocean Delta,” (Klausen et al., 2019) (Fig. 11B). The unconformities in red are the result of tectonic pulses caused by the Uralian-Pai-Khoi-Novaya Zemlya Orogeny on the eastern BSS region. So, as not to be mistaken for a tectophase-bounding unconformity, it is important to note that the green, Permo-Triassic unconformity in Figure 11B, used as a datum herein, is related to

regional uplift accompanying the Permo-Triassic super-plume event (Drachev, 2016), which was responsible for extrusion of the Siberian Traps in the West Siberian Basin (Saunders et al., 2007). In the rest of this section, we will examine the Late Permian–Middle Jurassic BSS cycles (Figs. 2, 3, 11B), considering the Appalachian Basin models pictured above (Figs. 8–11A).

As previously mentioned, the tectophase cycles are based on the presence of unconformities and a distinct overlying stratigraphic sequence (Fig. 8). In the Appalachian cycles, the basal unconformities and overlying succession typically become younger in space and time cratonward (Fig. 11A). Similarly, in the BSS, the first tectophase (Fig. 3; purple) is represented by the development of a basal Uralian unconformity in the east during Late Carboniferous (Bashkirian–Gzhelian) time (Fig. 3; col. 5, 6, 14), which migrates westward, becoming progressively younger into Early Permian (Kungurian) time (Fig. 3). Rocks on top of the basal unconformity are typically transgressive carbonates or black shales in Appalachian sections and represent rapid subsidence (Figs. 8, 10). Likewise, in the BSS section, Lower to Upper Permian (Kungurian–Wuchiapingian) deeper water carbonates and spiculites and Permo-Triassic black shales reflect transgression and rapid subsidence atop the unconformity (Figs. 2, 3, 11B), representing major deformational loading in the Uralides. Once loading halts, relaxation sets in and widespread erosion in the now uplifted orogen results in basin infilling with flysch-like clastics followed by molasse-like sediments, which are well observed in the Appalachian area (Figs. 8–11A). On the BSS, Late Carboniferous to Permian, deeper water, black shales do grade upward into flysch-like clastics of the Sassendal and lowermost Kapp Toscana groups (Figs. 2, 3, 11B), but at the Permo-Triassic transition, a prominent unconformity, most likely associated with regional uplift caused by the Permo-Triassic plume event, extensively truncates the section (Figs. 3, 11B). By Early Triassic (Induan) time, the unconformity is succeeded by

thick, molasse-like sedimentation, including marginal-marine, cyclically alternating, black shales and clastics with later fluvio-deltaic facies and coal (Fig. 3; 11B), suggesting local pulses of thrust movement in the nearby orogen like those noted in the Acadian section (Figs. 11A).

In the Appalachian Acadian sequence, the molasse-like sediments were deposited more proximally in the Catskill and Price-Pocono “Deltas” (Ettensohn, 2004). On the BSS, the very prominent molasse-like sequence comprises the “Triassic Boreal Ocean Delta” (Fig. 11B), which is purported to be the largest deltaic complex of its type in the Earth’s history (Klausen et al., 2019). These deltaic sequences were abruptly uplifted and capped by a Late Triassic, mid-Norian unconformity that signaled the advent of another tectophase, representing the advent of folding and thrusting of the Novaya Zemlya archipelago upon the BSS or the Novaya Zemlya Orogeny (Petrov et al., 2008; Henriksen et al., 2011). This tectophase (Fig. 3; orange) is represented by a typical sequence of organic-rich, flysch-like and molasse-like sediments and only lasted for about 20 m.y. from mid-Norian time to the Triassic-Jurassic boundary (Figs. 3, 11B). Rocks from this tectophase were abruptly truncated along a widespread, regional unconformity at the Triassic-Jurassic boundary (Figs. 3, 11B). This unconformity apparently characterizes the inception of another tectophase (Fig. 3; black), which represents the final transpressional collision and indentation of a segment of Siberian crust into Baltica in the Novaya Zemlya archipelago (Drachev et al., 2010; Curtis et al, 2018). Like the Alleghanian collisional orogeny (Fig. 5), this final collision generated a large wedge of alternating terrestrial and marginal-marine clastic sediments without lower parts of the cycle as in the Appalachian Basin (Table 2, Stage 7; Figs. 2, 3, 5). Sedimentation persisted for about 35 m. y. until Middle Jurassic (Bathonian) time, when uplift related to the opening of the Atlantic generated another unconformity (Figs. 3, 11B),

overlain by deep-water, Atlantic-type oceanic shales (Henriksen et al., 2011), which effectively terminated the Uralian-Pai-Khoi-Novaya Zemlya tectonostratigraphic succession on the BSS.

3.4 Intracratonic-basin analogues

Intracratonic basins are areas within the craton that have experienced broad, long-period, regional-scale sagging, with most lacking a rapid, initial subsidence phase (Klein and Hsui, 1987; Xie and Heller, 2009; Armitage and Allen, 2010). These basins are generally described as having sedimentary thicknesses of less than 5 km, and rarely 6–7 km, exhibiting a generally saucer-like geometry, lacking major syn-tectonic faults, and experiencing only occasional post-sedimentary faulting (Xie and Heller, 2009; Allen and Armitage, 2012). These characteristics are probably oversimplified because of the variety of subsidence mechanisms and geometries associated with these basins (Klein and Hsui, 1987; Ulmishek and Klemme, 1990; An and Assumpção, 2006; Ritzmann and Faleide, 2009; Armitage and Allen, 2010; Cloetingh and Burov, 2011; Gac et al., 2013). In the United States Illinois and Michigan basins (Fig. 1A), subsidence mechanisms are related to much earlier phases of rifting (Kolata and Nelson, 1991; McBride and Kolata, 1999), and subsequent flexural stresses associated with nearby orogenic activity (Cloetingh and Burov, 2011). Interestingly, Gac et al. (2013) concluded that the eastern BSS basins were largely formed by mechanisms like those forming the Illinois and Michigan basins, which were contemporaneous with Appalachian orogenies.

Stratigraphic successions in intracratonic basins are predominantly of terrestrial to shallow-water origin, which suggests that sedimentation effectively kept pace with subsidence (Allen and Armitage, 2012). Moreover, intracratonic stratigraphic successions can at times be tied to the development of adjacent foreland basins (Ettensohn, 1985, 1992) (Fig. 11A). In fact,

the same flexural stresses controlling foreland-basin sedimentation may also influence patterns of cratonic sedimentation some distance from the foreland basin, making it difficult to distinguish the intracratonic from the foreland tectonostratigraphic sequences (Ettensohn et al., 2019). Widespread source-rock deposition can also occur (Vyssotski et al., 2012), but some hydrocarbons in these basins may have originated in the adjacent foreland basin (Oliver, 1986; Sorokhtin et al., 2015).

In the Appalachian area, parts of various foreland-basin stratigraphic sequences migrated beyond the foreland basin into the adjacent intracratonic basins (Figs. 1A, 11A) (Ettensohn, 1992), intertonguing with local, intracratonic, stratigraphic sequences. Similarly, the Paleozoic to Mesozoic tectonostratigraphic sequence in the Novaya Zemlya foreland basin and eastern BSS basins (Figs. 1B, 2, 3, 11B) may represent foreland basin overfill and regional progradation of foreland tectonostratigraphic sequences far onto the adjacent craton, as in the Appalachian system (Fig. 11A). The persistent large-scale cratonward progradation of the Uralian-Pai-Khoi-Novaya Zemlya succession (Fig. 11B, southeastern Triassic–Jurassic clastic sequences) contributed to the filling of intracratonic basins in the western BSS and Russian-Norwegian BSS transitional areas (e.g., Olga and eastern Nordkapp basins; Figs. 1B, 2, 3, 11B), intertonguing with local intracratonic stratigraphic sequences.

Because of the several formation mechanisms possible (Allen and Armitage, 2012), the tectonostratigraphic nature of intracratonic basins can be unclear (Lindsay et al., 1993). However, based on work in the Appalachian area (e.g., Quinlan and Beaumont, 1984), it is also important to understand that some intracratonic basins may experience periodic interactions with adjacent foreland basins, resulting in periods of yoking (Ettensohn and Lierman, 2015) and intracratonic subsidence (Howell and van der Pluijm, 1990) related to orogenic activity in the

adjacent orogen. Hence, if development of intracratonic basins in the eastern BSS area is like that in the Appalachian area, as suggested by Gac et al. (2013) for the BSS, then processes from Appalachian intracratonic areas may well provide analogues, especially relative to subsidence rates (Smelror et al., 2009), fault reactivation (Anell et al., 2013), and foreland-basin-like stratigraphic successions on the BSS (Fig. 3).

4 SUMMARY

Using the features and history of a well-known area as analogues to understand a lesser-known area is a widely used technique in the geologic sciences and industry. Even though the studied areas may be widely separated and represent different times and places, external analogues may compensate for a lack of in-place data and provide new perspectives. Clearly, analogues are not perfect, but in areas of limited or unavailable knowledge, they should be examined as one of the first sources of information. To our knowledge, basin areas external to the Barents Sea shelf (BSS) and adjacent areas have not been widely used as analogues to the BSS. Inasmuch as both the Appalachian and BSS areas record the closure of an ocean or oceans and reflect the final stages of a Wilson cycle during the formation of Pangea, it is reasonable to expect the possibilities of at least large-scale analogues.

The main challenges in transposing Appalachian models to the BSS are the differences in timing, paleogeography, and paleoclimate. Even though the timing of tectonic events in the two areas is not the same, overall temporal differences should not affect the use of large-scale Appalachian analogues in the BSS area, because both areas experienced a very similar tectonic history. Similarly, the paleogeographic placement in time of both areas was not identical, but the succession of resulting paleoclimates in both areas was nearly the same and resulted in large-

scale clastic-carbonate-clastic successions, which broadly reflect a similar sequence of non-marine, marine, non-marine depositional settings. Moreover, both basins experienced times of rapid subsidence that led to the accumulation of thick stratigraphic sequences.

Assuming that Appalachian and BSS (Uralian) successions are tectonostratigraphically analogous and are largely the products of flexural interactions (loading and relaxation), then Appalachian tectonostratigraphic flexural models (e.g., tectophase cycles) should be applicable to the BSS. For example, using the Appalachian tectophase model merely transposes a Lower Permian-to-Jurassic succession of units on the BSS for a Lower-to-Upper Paleozoic successions of units in the Appalachian area. In this context, units from the Norwegian BSS would largely represent more distal cratonic areas, whereas units from the Russian BSS and Novaya Zemlya would constitute more proximal intracratonic, bulge-related, and foreland-basin areas. Hence, an Appalachian model effectively provides critical background when analyzing BSS regional unconformities, organic-rich rocks, petroleum systems, stratigraphic geometries, basin filling, correlation, tectonic timing and helps with integrating the regional tectonostratigraphy of both Norwegian and Russian BSS sectors.

The Paleozoic Appalachian succession is the result of complex interactions among foreland basins, intracratonic basins, platform systems and the widespread reactivation of Precambrian structures, which facilitated interactions between foreland and intracratonic basins. Similarly, the Upper Permian-to-Middle Jurassic BSS succession is the result of large-scale interactions among similar features of a younger age. In the BSS area, the Upper Paleozoic sequence generally begins with a major bounding unconformity, overlain in succession by organic-rich marine shales, flysch-like clastics, and molasse-like clastics, and is subsequently truncated by an unconformity. This succession is analogous to those in several Appalachian

foreland basins and adjacent intracratonic areas and is herein interpreted to be parts of unconformity-bound tectophase cycles related to flexural interactions with the orogen.

The large-scale setting with a deformed precursor basement, a closing ocean, a collisional orogen, and resulting foreland and intracratonic basins is much the same in both areas. What is new in this analysis is the recognition of tectonostratigraphic cycles in the BSS succession that reflect flexural responses typical of Appalachian tectophase cycles. The idea that the existing BSS stratigraphy can now be related to distinct phases of Uralian orogeny is relatively new and especially critical in understanding the BSS succession in a tectonostratigraphic framework. This understanding is clearly a product of using Appalachian tectonostratigraphic analogues and provides a foundation on which to develop the study of related BSS petroleum systems. This, we hope, will provide an additional tool for hydrocarbon exploration and in finding suitable carbon-capture and storage targets across the BSS.

(*Data sharing not applicable to this article as no datasets were generated or analyzed during the current study*).

REFERENCES

Abrams, M.A., Apanel, A.M., Timoshenko, O.M., and Kosenkova, N.N., 1999, Oil families and their potential sources in the northeastern Timan Pechora Basin, Russia: American Association of Petroleum Geologists Bulletin, v. 83, p. 553–577.

Alexander, J., 1993, A discussion on the use of analogues for reservoir geology, *in* Ashton, M., eds., Advances in Reservoir Geology: London, Geological Society Special Publication, v. 69, p. 175–194.

Allen, P.A., Crampton, S. L., and Sinclair, H. D., 1991, The inception and early evolution of the north Alpine foreland basin, Switzerland: Basin Research, v. 3, p. 143–163.

Allen, P.A., and Allen, J.R., 2013, Basin Analysis: Principles and application to petroleum play assessment: West Sussex, Wiley-Blackwell, 632 p.

Allen, P.A., and Armitage, J.J., 2012, Cratonic basins, *in* Busby, C., and Azor, A., eds., Tectonics of Sedimentary Basins: Recent Advances: West Sussex, Willey-Blackwell, p. 602–620.

Alsgaard, P.C., 1993, Eastern Barents Sea Late Palaeozoic setting and potential source rocks, *in* Vorren, T. O., Bergsager, E., Dahl-Stamnes, Ø.A., Holter, E., Johansen, B., Lie, E., and Lund, T.B., eds., Arctic Geology and Petroleum Potential: Amsterdam, NPF Special Publication, v. 2, p. 405–418.

Amantov, A., and Fjeldskaar, W., 2018, Meso-Cenozoic exhumation and relevant isostatic process: The Barents and Kara shelves: Journal Geodynamics, v. 118, p. 118–139.

An M., and Assumpção, M., 2006, Crustal and upper mantle structure in the intracratonic Paraná basin SE Brasil, from surface wave dispersion using genetic algorithms: Journal of South American Earth Sciences, v. 21, p. 173–184.

Anell, I., Braathen, A., Olaussen, S., and Osmundsen, P.T., 2013, Evidence of faulting contradicts a quiescent northern Barents shelf during the Triassic: First Break, v. 31, p. 67–76.

Anell, I., Braathen, A., and Olaussen, S., 2014, The Triassic–Early Jurassic of the northern Barents shelf: A regional understanding of the Longyearbyen CO2 reservoir: Norwegian Journal of Geology, v. 94, p. 83–98.

Anell, I., Faleide, J.I., and Braathen, A., 2016, Regional tectono-sedimentary development of the highs and basins of the northwestern Barents shelf: Norwegian Journal of Geology, v. 96, p. 27–41.

Armitage, J.J., and Allen, P.A., 2010, Cratonic basins and the long-term subsidence history of continental interiors: Journal of the Geological Society, v. 167, p. 61–70.

Arthaud, F., and Matte, P., 1977, Late Paleozoic strike-slip faulting in southern Europe and northern Africa: Result of a right-lateral shear zone between the Appalachians and the Urals: Geological Society of America Bulletin, v. 88, p. 1305–1320.

Artyushkov, E.V., and Baer, M.A., 1983, Mechanism of continental crust subsidence in fold belts: The Urals, Appalachians and Scandinavian Caledonides: Tectonophysics, v. 100, p. 5–42.

Artyushkov, E.V., and Baer, M.A., 1985, Mechanism of formation of deep basins in continental crust in fold belts: Journal of Geodynamics, v. 2, p. 67–84.

Artyushkov, E.V., and Baer, M.A., 1986, Mechanisms of formation of hydrocarbon basins: The West Siberia, Volga-Urals, Timan-Pechora basins and the Permian Basin of Texas: Tectonophysics, v. 122, p. 247–281.

Beaumont, C., 1981, Foreland basins: Geophysical Journal of the Royal Astronomical Society, v. 65, p. 291–329.

Blomeier, D., Scheibner, C., and Forke, H., 2009, Facies arrangement and cyclostratigraphic architecture of a shallow marine, warm-water carbonate platform: The Late Carboniferous Ny Friesland platform in eastern Spitsbergen (Pyefjellet Beds, Wordiekammen Formation, Gipsdalen Group): Facies, v. 55, p. 291–324.

Brekke, H., Sjulstad, H.I., Magnus, C., and Williams, R.W., 1999, Sedimentary environments offshore Norway — an overview, *in* Martinsen, O.J., and Dreyer, T., eds., Sedimentary Environments Offshore Norway – Palaeozoic to Recent: Bergen, Norwegian Petroleum Society, Special Publication, v. 10, p. 7–37.

Brown, D., Alvarez- Marron, J., Perez-Estaun, A., Gorozhanina, Y., and Puchkov, V., 2004, The structure of the South foreland fold and thrust belt at the transition of the Precaspian basin: Journal of the Geological Society, v. 161, p. 813–822.

Brown, D., Spadea, P., Puchkov, V., Alvarez-Marron, J., Herrington, R., Willner, A.P., Hetzel, R., Gorozhanina, Y., and Juhlin, C., 2006a, Arc–continent collision in the southern Urals: Earth-Science Reviews, v. 79, p. 261–287.

Brown, D., Puchkov, V., Alvarez-Marron, J., Bea, F., and Perez-Estaun, A., 2006b, Tectonic processes in the southern and middle Urals: an overview, *in* Gee, D.G., and Stephenson, R.A., eds., European Lithosphere Dynamics: London, The Geological Society of London, Memoirs, v. 32, p. 1–15.

Buiter, S.J.H., and Torsvik, T.H., 2007, Horizontal movements in the eastern Barents Sea constrained by numerical models and plate reconstructions: Geophysical Journal International, v. 171, p. 1376–1389.

Burguto, A.G., Zhuravlev, V.A., Zavarzina, G.A., and Zinchenko, A.G., 2016, State geological map of the Russian Federation (in Russian): Saint Petersburg, VSEGUEI, The North-Kara-Barents Sea series, Sheets S-36 and S-37, Scale 1: 1,000,000.

Camacho, A., Lee, J.K.W., Hensen, B.J., and Braun, J., 2005, Short-lived orogenic cycles and the eclogitization of cold crust by spasmodic hot fluids: Nature, v. 435, p. 1191–1196.

Coakley, B. J., and Watts, A. B., 1991, Tectonic controls on the development of unconformities: The North Slope, Alaska: Tectonics, v. 10, p. 101–130.

Cohen, K.M., Finney, S.C., Gibbard, P.L., and Fan, J.-X., 2013, The ICS International Chronostratigraphic Chart: v. 36, p. 199–204. Retrieved from https://stratigraphy.org/ICSchart/ChronostratChart2020-03.pdf

Colton, G.W., 1970, The Appalachian basin—Its depositional sequences and their geologic relationships *in* Fisher, G.W., Pettijohn, F.J., Reed, J.C., Jr., and Weaver, K.N., eds., Studies of Appalachian geology: Central and Southern: New York, Interscience Publishers, New York, p. 5–47.

Cloetingh, S., and Burov, E., 2011, Lithospheric folding and sedimentary basin evolution: A review and analysis of formation mechanisms: Basin Research, v. 23, p. 257–290.

Cluff, R.M., and Dickerson, D.R., 1982, Natural gas potential of the New Albany Shale group (Devonian-Mississippian) in southeastern Illinois: Society of Petroleum Engineers Journal, p. 291–300.

Coakley, B.J., and Watts, A.B., 1991, Tectonic controls on the development of unconformities: The North Slope, Alaska: Tectonics, v. 10, p. 101–130.

Corfu, F., Andersen, T.B., and Gasser, D., 2014, The Scandinavian Caledonides: main features, conceptual advances and critical questions, *in* Corfu, F., Gasser, D., and Chew, D.M., eds., New Perspectives on the Caledonides of Scandinavia and Related Areas: London, The Geological Society of London, Special Publications, v. 390, p. 9–43.

Curtis, J.B., and Faure, G., 1997, Accumulation of organic matter in the Rome trough of the Appalachian basin and its subsequent thermal history: American Association of Petroleum Geologists Bulletin, v. 81, p. 424–437.

Curtis, M.L., Lopez-Mir, B., Scott, R.A., and Howard, J.P., 2018, Early Mesozoic sinistral transpression along the Phai-Khoi-Novaya Zemlya fold–thrust belt, Russia, *in* Pease, V., and Coakley, B., eds., Circum-Arctic Lithosphere Evolution: London, Geological Society, Special Publications, v. 460, p. 355–370.

Dalland, A., Worsley, D. and Ofstad, K., 1988, A lithostratigraphical scheme for the Mesozoic and Cenozoic succession, offshore mid- and northern Norway: Stavanger, Norwegian Petroleum Directorate, v. 4, 65 p.

Dallmann, W.K., Blomeier, D., Elvevold, S., Mørk, A., Olaussen, S., Grundvåg, S.-A., Bond, D., and Hormes, A., 2015, Historical Geology, *in* Dallmann, W.K., eds., Geoscience Atlas of Svalbard: Tromsø, Norsk Plarinstitutt, v. 148, p. 89–181.

DeCelles, P.G., and Giles, K.A., 1996, Foreland basin systems: Basin Research, v. 8, p. 105–123.

Dedeev V. A., 1959, Interrelationships of the Polar Urals with neighboring folded regions (in Russia): Trudy VNIGRI, v. 126. Geology, p. 371–399.

Denison, R.E., 1989, Foreland structure adjacent to the Ouachita forebelt, *in* Hatcher, R.D., Jr., Thomas, W.A., and Viele, G.W., eds., The Appalachian-Ouachita Orogen in the United States, The Geology of North America: Boulder, Geological Society of America, v. F-2, p. 681–688.

Drachev, S.S., Malyshev, N.A., and Nikishin, A.M., 2010, Tectonic history and petroleum geology of the Russian Arctic shelves: an overview, *in* Vining, B.A., and Pickering, S.C., eds., Petroleum Geology Conferences: London, Geological Society of London, p. 591–619.

Drachev, S.S., 2016, Fold belts and sedimentary basins of the Eurasian Arctic: Arktos, v. 2, p. 1–30.

U.S. Energy Information Administration (EIA), 2021, Maps: Oil and Gas Exploration, Resources, and Production: Appalachian basin. Retrieved from https://www.eia.gov/maps/maps.htm?fbclid=IwAR2bc1KgMH2KXNdFoongJi7oZZJfv24E-D79WzjaXPulIy4OviJhiSnXxOU

Ershova, V.B., Prokopiev, A.V., and Khudoley, A.K., 2015, Integrated provenance analysis of Carboniferous deposits from northeastern Siberia: Implication for the late Paleozoic history of the Arctic: Journal of Asian Earth Sciences, v. 109, p. 38–49.

Ettensohn, F.R., 1985, The Catskill Delta complex and the Acadian Orogeny: A model, *in* Woodrow, D.L., and Sevon, W.D., eds., The Catskill Delta: Geological Society of America Special Paper 201, p. 39–49.

Ettensohn, F.R., 1991, Flexural interpretation of relationships between Ordovician tectonism and stratigraphic sequences, central and Southern Appalachians, U.S.A, *in* Barnes, C.R., and Williams, S.H., eds., Advances in Ordovician Geology: Geological Survey of Canada Paper 90-9, p. 213–224.

Ettensohn, F.R., 1992, Controls on the origin of the Devonian–Mississippian oil and gas shales, east-central United States: Fuel, v. 71, p. 1487–1492.

Ettensohn, F.R., 1997, Assembly and dispersal of Pangea: Large-scale tectonic effects on coeval deposition of North American, marine, epicontinental black shales: Journal of Geodynamics, v. 23, p. 287–309.

Ettensohn, F.R., 2004, Modeling the nature and development of major Paleozoic clastic wedges in the Appalachian basin, USA: Journal of Geodynamics, v. 37, p. 657–681.

Ettensohn, F.R., 2008, Chapter 4: The Appalachian foreland basin in eastern United States, *in* Miall, A., eds., The Sedimentary Basins of the United States and Canada: Sedimentary Basins of the World: Amsterdam, Elsevier, p. 105–179.

Ettensohn, F.R., and Lierman, R.T., 2012, Chapter 4, Large-scale tectonic controls on the origin of Paleozoic, dark shale, source-rock basins: Examples from the Appalachian foreland-basin region, eastern United States, *in* Gao, D., eds., Tectonics and Sedimentation: Implications for Petroleum Systems: American Association of Petroleum Geologists Memoir 100, p. 95–124.

Ettensohn, F.R., and Lierman, R.T., 2015, Using black shales to constrain possible tectonic and structural influence on foreland-basin evolution and cratonic yoking: Late Taconian Orogeny, Late Ordovician Appalachian Basin, eastern USA, *in* Gibson, G.M, Roure, F., and Manatschal, G., eds., Sedimentary basins and crustal processes at continental margins: From hyper-extended margins to deformed ancient analogues: Geological Society of London Special Publication 413, p. 119–141.

Ettensohn, F.R., Lierman, R.T., Udgata, D.B.P., and Mason, C.E., 2012, The Early-Middle Mississippian Borden Grainger–Fort Payne delta/basin complex: Field evidence for delta sedimentation, basin starvation, mud-mound genesis, and tectonism during the Neoacadian Orogeny, *in* Eppes, M.C., and Bartholomew, M.J., eds., From the Blue Ridge to the Coastal Plain: Field Excursions in the Southeastern United States: Geological Society of America Field Guide, v. 29, p. 345–395,

Ettensohn, F.R., Pashin, J.C., and Gilliam, W., 2019, The Appalachian and Black Warrior Basins: Foreland basins in the eastern United States, *in* Miall, A., eds., The Sedimentary basins of the United States and Canada: Sedimentary Basins of the World: Amsterdam, Elsevier, p. 129–237.

Faleide, J.I., Gudlaugsson, S.T., and Jacquart, G., 1984, Evolution of the western Barents Sea: Marine and Petroleum Geology, v. 1, p. 123–150.

Faleide, J.I., Tsikalas, F., Breivik, A.J., Mjelde, R., Ritzmann, O., Egen, Ø., Wilson, J., and Eldholm, O., 2008, Structure and evolution of the continental margin off Norway and the Barents Sea: Episodes, v. 31, p. 82–91.

Faleide, J.I., Pease, V., Curtis, M., Klitzke, P., Minakov, A., Scheck-Wenderoth, M., Kostyuchenko, S., and Zayonchek, A., 2017, Tectonic implications of the lithospheric structure across the Barents and Kara shelves, *in* Pease, V., and Coakley, B., eds., Circum-Arctic Lithosphere Evolution: London, Geological Society of London, Special Publications, v. 460, p. 285–314.

Finney, S.C., Grubb, B.J., and Hatcher, R.D., Jr., 1996, Graphic correlation of Middle Ordovician graptolite shale, southern Appalachians: an approach for examining the subsidence and migration of a Taconic foreland basin: Geological Society of America Bulletin, v. 108, p. 355–371.

Filatova, N.I., and Khain, V.E., 2010, The Arctida craton and Neoproterozoic–Mesozoic orogenic belts of the circum–polar region: Geotectonics, v. 44, p. 203–227.

Gac, S., Huismans, R.S., Simon, N.S.C., Podladchikov, Y.Y., and Faleide, J.I., 2013, Formation of intracratonic basins by lithospheric shortening and phase changes: a case study from ultra-deep East Barents Sea basin: Terra Nova, v. 25, p. 459–463.

Gao, D., Shumaker, R.C., and Wilson, T.H., 2000, Along-axis segmentation and growth history of the Rome Trough in the central Appalachian Basin: American Association of Petroleum Geologists Bulletin, v. 84, p. 75–99.

Gee, D. G., 2005, Timanides of Northern Russia, *in* Selley, R.C., Cocks, L.R.M., and Plimer, I.R., eds., Encyclopedia of Geology: Amsterdam, Elsevier, V. 2, p. 64–74.

Gee, D.G., Bogolepova, O.K., and Lorenz, H., 2006, The Timanide, Caledonide and Uralide orogens in the Eurasian high arctic, and relationships to the palaeo-continents Laurentia, Baltica and Siberia, *in* Gee, D.G., and Stephenson, R.A., European Lithosphere Dynamics: London, Geological Society, v. 32, p. 507–520.

Gee, D.G., Fossen, H., Henriksen, N., and Higgins, A.K., 2008, From the Early Paleozoic platforms of Baltica and Laurentia to the Caledonide Orogen of Scandinavia and Greenland: Episodes, v. 31, p. 44–51.

Gee, D.G., Juhlin, C., Pascal, C, and Robinson, P., 2010, Collisional orogeny in the Scandinavian Caledonides: GFF, v. 132, p. 29–44.

Georgiev, S.V., Stein, H.J., Hannah, J.L., Xu, G., Bingen, and Weiss, H.M., 2017, Timing, duration, and causes for Late Jurassic–Early Cretaceous anoxia in the Barents Sea: Earth and Planetary Science Letters, v. 461, p. 151–162.

Gernigon, L., Brönner, M., Roberts, D., Olesen, O., Nasuti, A., and Yamasaki, T., 2014, Crustal and basin evolution of the southwestern Barents Sea: From Caledonian Orogeny to continental breakup: Tectonics, v. 33, p. 347–373.

Gernigon, L., Brönner, M., Dumais, M.-A., Gradmann, S., Grønlie, A., Nasuti, A., and Roberts, D., 2018, Basement inheritance and salt structures in the SE Barents Sea: Insights from new potential field data: Journal of Geodynamics, v. 119, p. 82–106.

Golonka, J., and Ford, D., 2000, Pangean (Late Carboniferous–Middle Jurassic) paleoenvironment and lithofacies: Palaeogeography, Palaeoclimatology, Palaeoecology, v. 161, p. 1–34.

Greb, S.F., Pashin, J.C., Martino, R.L., and Eble, C.F., 2008, Appalachian sedimentary cycles during the Pennsylvanian: Changing influences of sea level, climate, and tectonics, *in* Fielding, C.R., Frank, T.D., and Isbell, J.L., eds., Resolving the Late Paleozoic Ice Age in Time and Space: Geological Society of America Special Paper 441, p. 235–248.

Grogan, P., Østvedt-Ghazi, A.-M., Larssen, G.B., Fotland, B., Nyberg, K., Dahlgren, S., and Eidvin, T., 1999, Structural elements and petroleum geology of the Norwegian sector of the northern Barents Sea, *in* Fleet, A.J., and Boldy, S.A.R., eds., Petroleum Geology of Northwest Europe: Proceedings of the 5th Conference: London, the Geological Society, v. 1, 247–259 p.

Guo, L., Schekoldin, R., and Scott, R., 2010, The Devonian succession in northern Novaya Zemlya, Arctic Russia: Sedimentology palaeogeography and hydrocarbon occurrence: Journal of Petroleum Geology, v. 33, p. 105–122.

Hatcher, R.D., Jr., 2010, The Appalachian orogen: A brief summary, *in* Tollo, R.P., Bartholomew, M.J., Hibbard, J.P., and Karabinos, P.M., eds., From Rodinia to Pangea: The Lithotectonic Record of the Appalachian Region, Geological Society of America Memoir, v. 206, p. 1–19.

Hatcher, R.D., Jr., Thomas, W.A., Geiser, P.A., Snoke, A.W., Mosher, S., and Wiltschko, D.V., 1989, Chapter 5, Alleghanian orogen, *in* Hatcher, R.D., Jr., Thomas, W.A., and Viele, G.W., eds., The Appalachian-Ouachita Orogen in the United States, The Geology of North America: Boulder, Geological Society of America, v. F-2, p. 233–318.

Hatcher, R.D., Jr., Bream, B.R., and Merschat, A.J., 2007, Tectonic map of the southern and central Appalachians: A tale of three orogens and a complete Wilson cycle, *in* Hatcher, R.D., Jr., Carlson, M.P., McBride, J.H., and Martínez Catalan, J.R., eds., 4-D Framework of Continental Crust: Geological Society of America Memoir, v. 200, p. 595–632.

He, M., Moldowan, J.M., Nemchenko-Rovenskaya, A., and Peters, K.E., 2012, Oil families and their inferred source rocks in the Barents Sea and northern Timan-Pechora Basin, Russia: American Association of Petroleum Geologists Bulletin, v. 96, p. 1121–1146.

Henriksen, E., Ryseth, A.E., Larssen, G.B., Heide, T., Rønning, K., Sollid, K., and Stoupakova, A.V., 2011, Tectonostratigraphy of the greater Barents Sea: Implications for petroleum systems, *in* Spencer, A.M., Embry,

A.F., Gautier, D.L., Stoupakova, A., and Sørensen, K., eds., Arctic Petroleum Geology: London, Geological Society, Memoirs, v. 35, p. 163–195.

Howell, P.D., and van der Pluijm, B.A., 1990, Early history of the Michigan Basin: Subsidence and Appalachian tectonics: Geology, v. 18, p.1195–1198.

Howell, J.A., Martinius, A.W., and Good, T.R., 2014, The application of outcrop analogues in geological modelling: a review, present status and future outlook, *in* Martinius A.W., Howell, J.A., and Good, T.R., eds., Sediment-body geometry and heterogeneity: Analogue studies for modelling the subsurface: London, Geological Society, Special Publications, v. 387, p. 1–25.

Ivanova, N.M., 1997, Prospective Paleozoic reefs in the southern part of the Barents Sea shelf: Petroleum Geoscience, v. 3, p. 153–160.

Ivanova, N.M., Sakoulina, T.S., and Roslov, Yu, V., 2006, Deep seismic investigations across the Barents–Kara region and Novozemelskiy fold belt (Arctic shelf): Tectonophysics, v. 420, p. 123– 140.

Jamieson, R.A., and Beaumont, C., 1988, Orogeny and metamorphism: A model for deformation and pressure-temperature-time paths with applications to the central and southern Appalachians: Tectonics, v. 7, p. 417–445.

Johansen, S.E., Ostisty, B.K., Birkeland, Ø, Federovsky, Y.F., Martirosjan, V.N., Bruun Christensen, O., Cheredeevm S.I., Ignatenko, E.A., and Margulis, L.S., 1993, Hydrocarbon potential in the Barents Sea region: play distribution and potential, *in* Vorren, T.O., Bergsager, E., Dahl-Stamnes, Ø.A., Holter, E., Johansen, B., Lie, E., and Lund, T.B., eds., Arctic Geology and Petroleum Potential: Amsterdam, Elsevier, v. 2, p. 273–320.

Johnson, J.G., 1971, Timing and coordination of orogenic, epeirogenic, and eustatic events: Geological Society of America Bulletin, v. 82, p. 3263–3298.

Klausen, T.G., Nyberg, B., and Helland-Hansen, W., 2019, The largest delta plain in Earth's history: Geology, v. 47, p. 470–474.

Klein, G.de V., and Hsui, A.T., 1987, Origin of cratonic basins: Geology, v. 15, p. 1094–1098.

Klett, T.R., and Pitman, J.K., 2011, Geology and petroleum potential of the East Barents Sea basins and Admiralty High, *in* Spencer, A.M., Embry, A.F., Gautier, D.L., Stoupakova, A., and Sørensen, K., eds., Arctic Petroleum Geology: London, Geological Society, Memoirs, v. 35, p. 295–310.

Klitzke, P., Faleide, J.I., Scheck-Wenderoth, M., and Sippel, J., 2015, A lithosphere-scale structural model of Barents Sea and Kara Sea region: Solid Earth, v. 6, p. 153–172.

Klitzke, P., Franke, D., Ehrhardt, A., Lutz, R., Reinhardt, L., Heyde, I., and Faleide, J.I., 2019, The Paleozoic evolution of the Olga Basin region, northern Barents Sea: A link to the Timanian Orogeny: Geochemistry, Geophysics, Geosystems, v. 20, p. 1–16.

Knapp, J.H., Diaconescu, C.C., Bader, M.A., Sokolov, V.B., Kashubin, S.N., and Rybalka, A.V., 1998, Seismic reflection fabrics of continental collision and post-orogenic extension in the middle Urals, central Russia: Tectonophysics, v. 288, p. 115–126.

Knutsen, S.-M., and Larsen, K.I., 1997, The late Mesozoic and Cenozoic evolution of the Sørvestsnaget Basin: A tectonostratigraphic mirror for regional events along the southwestern Barents Sea margin: Marine and Petroleum Geology, v. 14, p. 27–54.

Kolata, D.R., and Nelson, W.J., 1991, Tectonic history of the Illinois basin, *in* Leighton, M.W., Kolata, D.R., Oltz, D.F., and Eidel, J.J., eds., Interior Cratonic Basins: Tulsa, American Association of Petroleum Geologists, Memoir 51, p. 263–285.

Konyukhov, A.I., 2014, Hydrocarbon source rocks in sedimentary basins of continental margins in the Middle–Late Paleozoic: Lithology and Mineral Resources, v. 49, p. 336–358.

Konyukhov. A.I., 2016, Black shales and other sediments with high organic matter contents in Phanerozoic climatic cycles: Communication 2. Black shales during the Pangea existence: Lithology and Mineral Resources, v. 51, p. 42–67.

Kruse, S., and McNutt, M., 1988, Compensation of Paleozoic orogens: a comparison of the Urals to the Appalachians: Tectonophysics, v. 154, p. 1–17.

Kuznetsov, N.B., 2006, The Cambrian Baltica–Arctida Collision, Pre-Uralide–Timanide Orogen, and its erosion products in the Arctic: Doklady Earth Sciences, v. 411A, p. 1375–1380.

Larssen, G.B., Elvebakk, G., Henriksen, L.B., Kristensen, S.-E., Nilsson, I., Samuelsberg, T.J., Svånå, T.A., Stemmerik, L., and Worsley, D., 2002, Upper Paleozoic lithostratigraphy of the southern Norwegian Barents Sea: Norwegian Petroleum Directorate, 76 p.

Leonchik M.I., and Senin, B.V., 2010, Oil potential prospects for Paleozoic carbonates in the Russian sector of the Barents Sea (in Russian): Neftegasovaâ Geologiâ, Teoriâ i Practika, v. 5, p. 1–16.

Lindsay, J.F., Kennard, J.M., and Southgate, P.N., 1993, Application of sequence stratigraphy in an intracratonic setting, Amadeus Basin, central Australia, *in* Posamentier, H.W., Summerhayes, C.P., Haq, B.U., and Allen,

G.P., eds., Sequence Stratigraphy and Facies Associations: Cambridge, Blackwell Scientific Publications, v.18, p. 605–631.

Lopatin, B.G., Pavlov, L.G., Orgo, V. V., Shkarubo, S.I., 2001, Tectonic structure of Novaya Zemlya: Polarforschung, v. 69, p. 131–135.

Lopatin, N.V., Zubairaev, S.L., Kos, I.M., Emets, T.P., Romanov, E.A., and Malchikhina, O.V., 2003, Unconventional oil accumulations in the Upper Jurassic Bazhenov black shale formation, West Siberian basin: a self-sourced reservoir system: Journal of Petroleum Geology, v. 26, p. 225–244.

Lopes, G., Mangerud, G., Clayton, G., and Mørk, A., 2016, New insights on East Finnmark Platform palynostratigraphy and paleogeography – A study of three shallow cores from a Mississippian succession in the Barents Sea, Norway: Palaeogeography, Palaeoclimatology, Palaeoecology, v. 450, p. 60–76.

Lundschien, B.A., Høy, T., and Mørk, A., 2014, Triassic Hydrocarbon potential in the northern Barents Sea; integrating Svalbard and stratigraphic core data, *in* Mørk, A., Lundschien, B.A., and Høy, T., eds., Norwegian Petroleum Directorate Bulletin No.11: Stavanger, Norwegian Petroleum Directorate, v. 11, p. 3–20.

Marello, L., Ebbing, J., and Gernigon, L., 2013, Basement inhomogeneities and crustal setting in the Barents Sea from a combined 3D gravity and magnetic model: Geophysical Journal International, v. 193, p. 1–29.

Margulis, E.A., 2008, Factors of formation of a unique Shtokmanovsky-Ludlovsky gas accumulation node in the Barents Sea (in Russian): Neftegasovaâ Geologiâ, Teoriâ i Practika, v. 3, p. 1–15.

Matte, P., 2002, Variscides between Appalachians and the Urals: Similarities and differences between Paleozoic subduction and collision belts: Geological Society of America, Special Paper, v. 364, p. 1–13.

Matysik, M., Stemmerik, L., Olaussen, S., and Brunstad, H., 2018, Diagenesis of spiculites and carbonates in a Permian temperate ramp succession – Tempelfjorden Group, Spitsbergen, Arctic Norway: Sedimentology, v. 65, p. 745–774.

McBride, J.H., and Kolata, D.R., 1999, Upper crust beneath the central Illinois basin: Geological Society of America Bulletin, v. 111, p. 375–394.

McKerrow, W.S., Mac Niocaill, C., and Dewey, J.F., 2000, The Caledonian Orogeny redefined: Journal of the Geological Society, v. 157, p. 1149–1154.

Miall, A.D., and Blakey, R.C., 2019, The Phanerozoic tectonic and sedimentary evolution of North America, *in* Miall, A., eds., The Sedimentary basins of the United States and Canada: Sedimentary Basins of the World: Amsterdam, Elsevier, p. 1–38.

Müller, R., Klausen, T.G., Faleide, J.I., Olaussen, S., Eide, C.H., and Suslova, A., 2019, Linking regional unconformities in the Barents Sea to compression-induced forebulge uplift at the Triassic-Jurassic transition: Tectonophysics, v. 765, p. 35–51.

Nakrem, H.A., 2007, The 1921 O. Holtedahl Novaya Zemlya collection – geology (illustrated atlas): Oslo, Novazem, 31 p.

Nicolaisen, J.B., Elvebakk, G., Ahokas, J., Bojesen-Koefoed, J.A., Olaussen, S., Rinna, J., Skeie, J.E., and Stemmerik, L., 2019, Characterization of upper Palaeozoic organic-rich units in Svalbard: implications for the petroleum systems of the Norwegian Barents shelf: Journal of Petroleum Geology, v. 42, p. 59–78.

Nikishin, A.M., Ziegler, P.A., Stephenson, R.A., Cloetingh, S.A.P.L., Furne, A.V., Fokin, P.A., Ershov, A.V., Bolotov, S.N., Korotaev, M.V., Alekseev, A.S., Gorbachev, V.I., Shipilov, E.V., Lankreijer, A., Bembinova, E.Yu., and Shalimov, I.V., 1996, Late Precambrian to Triassic history of the East European Craton: Dynamics of sedimentary basin evolution: Tectonophysics, v. 268, p. 23–63.

Nikishin A.M., Ziegler, P.A., Abbott, D., Brunet, M.-F., and Cloetingh, S., 2002, Permo–Triassic intraplate magmatism and rifting in Eurasia: implications for mantle plumes and mantle dynamics: Tectonophysics, v. 351, p. 3–39.

Norina, D.A., Stupakova, A.V., and Kiryukhina, T.A., 2014, Depositional environments and the hydrocarbon generative potential of Triassic rocks of the Barents Sea basin: Moscow University Geology Bulletin, v. 69, p. 1–10.

Norwegian Petroleum Directorate (NPD), 2017, The Barents Sea North. Geological assessment of petroleum resources in eastern parts of Barents Sea North: Stavanger, Norwegian Petroleum Directorate, 39 p.

Norwegian Petroleum Directorate (NPD), 2021, Structural elements and fault lineaments of the Barents Sea shelf. Retrieved from https://www.npd.no/en/about-us/information-services/open-data/

Olaussen, S., Larssen, G.B., Helland-Hansen, W., Johannessen, E.P., Nøttvedt, A., Riis, F., Rismyhr, B., Smelror, M., and Worsley, D., 2018, Mesozoic strata of Kong Karls Land, Svalbard, Norway; a link to the northern Barents Sea basins and platforms: Norwegian Journal of Geology, v. 98, p. 1–70.

Ohm, S.E., Karlsen, D.A., and Austin, T.J.F., 2008, Geochemically driven exploration models in uplifted areas: examples from the Norwegian Barents Sea: American Association of Petroleum Geologists Bulletin, v. 92, p. 1191–1223.

O'Leary, N., White, N., Tull, S., Bashilov, V., Kuprin, V., Natapov, L., and Macdonald, D., 2004, Evolution of the Timan-Pechora and South Barents Sea basins: Geological Magazine, v. 141, p. 141–160.

Oliver, J., 1986, Fluids expelled tectonically from orogenic belts: Their role in hydrocarbon migration and other geologic phenomena: Geology, v. 14, p. 99–102.

Otto S.C., and Bailey, R.J., 1995, Tectonic evolution of the northern Ural Orogen: Journal of the Geological Society, v. 152, p. 903–906.

Park, H., Barbeau Jr, D.L., Rickenbaker, A., Bachmann-Krug, D., and Gehrels, G., 2010, Application of foreland basin detrital-zircon geochronology to the reconstruction of the southern and central Appalachian orogen: The Journal of Geology, v. 118, p. 23–44.

Pease, V., Drachev, S., Stephenson, R., and Zhang, X., 2014, Arctic lithosphere – A review: Tectonophysics, v. 628, p. 1–25.

Petrov, O.V., Sobolev, N.N., Koren, T.N., Vasiliev, V.E., Petrov, E.O., Larssen, G.B., and Smelror, M., 2008, Palaeozoic and Early Mesozoic evolution of the East Barents and Kara Seas sedimentary basins: Norwegian Journal of Geology, v. 88, p. 227–234.

Petrov, O.V., Mozorov, A., Shokalsky, S., Kashubin, S., Artemieva, I.M., Sobolev, N., Petrov, E., Ernst, R.E., Sergeev, S., and Smelror, M., 2016, Crustal structure and tectonic model of the Arctic region: Earth-Science Reviews, v. 154, p. 29–71.

Polyakova, I.D., 2015, Petroleum source rocks of the arctic region: Lithology and Mineral Resources, v. 50, p. 26–49.

Price, R.A., 1973, Large-scale gravitational flow of supracrustal rocks, southern Canadian Rockies, *in* de Jong, K.A., and Scholten, R., eds., Gravity and Tectonics: New York, John Wiley, p. 491–502.

Prischepa, O.M., Bazhenova, T.K., and Bogatskii, V.I., 2011, Petroleum systems of the Timan-Pechora sedimentary basin (including the offshore Pechora Sea): Russian Geology and Geophysics, v. 52, p. 888–905.

Proust, J.N., Chuvasov, B.I., Vennin, E., and Boisseau, T., 1998, Carbonate platform drowning in a foreland setting: The Mid-Carboniferous platform in western Urals (Russia): Journal of Sedimentary Research, v. 68, p. 1175–1188.

Puchkov, V.N., 1997, Structure and geodynamics of the Uralian orogen, *in* Burg, J.P., and Ford, M., eds., Orogeny through Time: London, The Geological Society of London, Geological Society Special Publication, v. 121, p. 201–236.

Puchkov, V.N., 2002, Paleozoic evolution of the East European continental margin involved in the Uralide Orogeny, *in* Brown, D., Juhlin, C., and Puchkov, V., eds., Mountain Building in the Uralides: Washington DC, American Geophysical Union, Geophysical Monograph, v. 132, p. 9–31.

Puchkov, V. N., 2003, Uralides and Timanides: their structural relationship and position in the geologic history of the Ural-Mongolian fold belt: Russian Geology and Geophysics, v. 44, p. 28–39.

Puchkov, V.N., 2009, The evolution of the Uralian Orogeny: Geological Society, London, Special Publications, v. 327, p. 161–195.

Puchkov, V.N., and Ivanov, K.S., 2020, Tectonics of the northern Urals and Western Siberia: General history of development: Geotectonics, v. 54, p. 35–53.

Quinlan, G.M., and Beaumont, C., 1984, Appalachian thrusting, lithospheric flexure, and the Paleozoic stratigraphy of the eastern interior of North America: Canadian Journal of Earth Sciences, v. 21, p. 973–996.

Rafaelsen, B., Elvebakk, G., Andreassen, K., Stemmerik, L., Colpaert, A., and Samuelsberg, T.J., 2008, From detached to attached carbonate buildup complexes – 3D seismic data from the upper Palaeozoic, Finnmark platform, southwestern Barents Sea: Sedimentary Geology, v. 206, p. 17–32.

Reid, C.M., James, N.P., Beauchamp, B., and Kyser, T.K., 2007, Faunal turnover and changing oceanography: Late Paleozoic warm-to-cool water carbonates, Sverdrup basin, Canadian Arctic Archipelago: Palaeogeography, Palaeoclimatology, Palaeoecology, v. 249, p. 128–159.

Repetski, J.E., Robert T.R., Anita G.H., and Michael H.T., 2008, Thermal maturity patterns (CAI and $\%R_o$) in Upper Ordovician and Devonian rocks of the Appalachian Basin: A major revision of USGS Map I-917-E using new subsurface collections: United States Geological Survey, Scientific Investigations Map 3006, 26 p.

Riis, F., Lundschien, B.A., Høy, T., Mørk, A., and Mørk, M.B., 2008, Evolution of the Triassic shelf in the northern Barents Sea region: Polar Research, v. 27, p. 318–338.

Ritzmann, O., and Faleide, J.I., 2009, The crust and mantle lithosphere in the Barents Sea/Kara Sea region: Tectonophysics, v. 470, p. 89–104.

Roen, J.B., 1984, Geology of the Devonian black shales of the Appalachian basin: Organic Geochemistry, v. 5, p. 241–254.

Ryseth, A., Augustson, J.H., Charnock, M., Haugerud, O., Knutsen, S.-M., Midbøe, P.S., Opsal, J.G., and Sundsbø, G., 2003, Cenozoic stratigraphy and evolution of the Sørvestsnaget Basin, southwestern Barents Sea: Norwegian Journal of Geology, v. 83, p. 107–130.

Saunders, A.D., Jones, S.M., Morgan, L.A., Pierce, K.L., Widdowson, M., and Xu, Y.G., 2007, Regional uplift associated with continental large igneous provinces: The roles of mantle plumes and the lithosphere: Chemical Geology, v. 241, p. 282–318.

Schellart, W.P., and Strak, V., 2016, A review of analogue modelling of geodynamic processes: Approaches, scaling, materials and quantification, with an application to subduction experiments: Journal of Geodynamics, v. 100, p. 7–32.

Schenk, C.J., 2011, Geology and petroleum potential of the Timan-Pechora basin province, Russia, The geological evolution and hydrocarbon potential of the Barents and Kara shelves, *in* Spencer, A.M., Embry, A.F., Gautier, D.L., Stoupakova, A.V., Sørensen, K., eds., Arctic Petroleum Geology: London, The Geological Society of London Memoirs, v. 35, p. 283–294.

Scott, R.A., 2007, Eastern Barents Sea-Novaya Zemlya-Kara Sea tectonic relationships: the search for an appropriate analogue: CASP Report, Cambridge, 50 p.

Scott, R.A., Howard, J.P., Guo, L., Schekoldin, R., and Pease, V., 2010, Offset and curvature of the Novaya Zemlya fold-and-thrust belt, Arctic Russia, *in* Vining, B.A., and Pickering, S.C., eds., Petroleum Geology: From Mature Basins to New Frontiers – Proceedings of the 7th Petroleum Geology Conference: London, The Geological Society, Petroleum Geology Conferences, v. 7, p. 645–657.

Serck, C.S., Faleide, J.I., Braathen, A., Kjølhamar, B., and Escalona, A., 2017, Jurassic to Early Cretaceous basin configuration(s) in the Fingerdjupet subbasin, SW Barents Sea: Marine and Petroleum Geology, v. 86, p. 874–891.

Shipilov, E.V., 2010, Role of the tectonomagmatic factor in formation of giant hydrocarbon accumulations in the East Barents Basin: Doklady Earth Sciences, v. 434, p. 1298–1302.

Sims, P.K., Saltus, R.W., and Anderson, E.D., 2008, Precambrian basement structure map of the continental United States—An interpretation of geologic and aeromagnetic data: U.S. Geological Survey Scientific Investigations Map 3012, scale: 1:8,000,000.

Sinclair, H.D., Coakley, B. J., Allen, P. A., and Watts, A. B., 1991, Simulation of foreland basin stratigraphy using a diffusion model of mountain belt uplift and erosion: an example from the central Alps, Switzerland: Tectonics, v. 10, p. 599–620.

Sloss, L.L., 1963, Sequences in the cratonic interior of North America: Geological Society of America Bulletin, v. 74, p. 93–114.

Smelror, M., and Petrov, O.V., 2018, Geodynamics of the Arctic: From Proterozoic orogens to present day seafloor spreading: Journal of Geodynamics, v. 121, p. 185–204.

Smelror, M., Petrov, O.V., Larssen, G.B., and Werner, S.C., 2009, Geological history of the Barents Sea: Trondheim, Geological Survey of Norway, 135 p.

Sorokhtin, N.O., Lobkovsky, L.I., Kozlov, N.E., Novikov, N.G., Nikiforov, S.L., and Bogdanova, O.Y., 2015, Evolution of the Barents Sea basin and oil and gas potential of coastal zones in the Kola region: Doklady Earth Sciences, v. 465, p. 1229–1232.

Stemmerik L., 2000, Late Palaeozoic evolution of the North Atlantic margin of Pangea. Palaeogeography, Palaeoclimatology, Palaeoecology, v. 161, 95–126.

Stemmerik, L., and Worsley, D., 2005, 30 years on – Arctic Upper Palaeozoic stratigraphy, depositional evolution and hydrocarbon prospectivity: Norwegian Journal of Geology, v. 85, p. 151–168.

Stemmerik, L., Christiansen, F. G., Piasecki, S., Jordt, B., Marcussen, C., and Nøhr-Hansen, H., 1993, Depositional history and petroleum geology of the Carboniferous to Cretaceous sediments in the northern part of East Greenland, *in* Vorren, T.O., Bergsager, E., Dahl-Stamnes, Ø.A., Holter, E., Johansen, B., Lie, E., and Lund, T.B., eds., Arctic Geology and Petroleum Potential: Amsterdam, Elsevier, v. 2, p. 273–320.Stemmerik, L., Larson, P.A., Larssen, G.B., Mørk, A., and Simonsen, B.T., 1994, Depositional evolution of Lower Permian *Palaeoaplysina* build-ups, Kapp Duner Formation, Bjørnøya, Arctic Norway: Sedimentary Geology, v. 92, p. 161–174.

Stephenson, R.A., Yegorova, T., Brunet, M.-F., Stovba, S., Wilson, M., Starostenko, V., Saintot, A., and Kuznir, N., 2006, Late Palaeozoic intra- and pericratonic basins on the East European Craton and its margins, *in* Gee, D.G.,

and Stephenson, R.A., eds., European Lithosphere Dynamics: London, The Geological Society of London, Memoirs, v. 32, p. 463–479.

Stockmal, G.S., Slingsby, A., and Waldron, J.W.F., 1998, Deformation styles at the Appalachian structural front, western Newfoundland: implications of new industry seismic reflection data: Canadian Journal of Earth Sciences, v. 35, p. 1288–1306.

Stoupakova, A.V., Henriksen, E., Burlin, Yu.K., Larsen, G. B., Milne, J.K., Kiryukhina, T.A., Golynchik, P.O., Bordunov, S.I., Ogarkova, M.P., and Suslova, A.A., 2011, The geological evolution and hydrocarbon potential of the Barents and Kara shelves, *in* Spencer, A.M., Embry, A.F., Gautier, D.L., Stoupakova, A.V., Sørensen, K., eds., Arctic Petroleum Geology: London, The Geological Society of London, Memoirs, v. 35, p. 325–344.

Stoupakova, A.V., Fadeeva, N.P., Kalmykov, G.A., Bogomolov, A.Kh., Kiryukhina, T.A., Korobova, N.I., Shardanova, T.A., Suslova, A.A., Sautkin, R.S., Poludektina, E.N., Kozlova, E.V., Mitronov, D.V., and Korkots, F.V., 2015, Criteria for oil and gas search in domanic deposits of the Volga-Ural basin (in Russian): Georesursy, v. 2, p. 77–86.

Stupakova, A.V., Suslova, A.A., Korobova, N.I., and Burlin, Yu.K., 2012, Cyclicity and prospects of the Jurassic oil-and-gas complex on the Barents Sea shelf: Moscow University Geology Bulletin, v. 67, p. 353–360.

Su, W., Huff, W.D., Ettensohn, F.R., Liu, X., Zhang, J., and Li, Z., 2009, K-bentonite, black-shale and flysch successions at the Ordovician-Silurian transition, South China: Possible sedimentary responses to the accretion of Cathaysia to the Yangtze Block and its implications for the evolution of Gondwana: Gondwana Research, v. 15, p. 111–130.

Sun, S., Politt, D.A., Wu, S., and Leary, D.A., 2021, Use of global analogues to improve decision quality in exploration, development and production: American Association of Petroleum Geologists Bulletin, v. 105, p. 845–864.

Suvorova, E.B., and Matveeva, T.V., 2014, Lithofacies features of Carboniferous–Lower Permian strata from the Pechora Sea, *in* Stone, D.B., Grikurov, G.E., Clough, J.G., Oakey, G.N., and Thurston, D.K., eds., Proceedings of the International Conference on Arctic Margins VI: Saint Petersburg, VSEGEI, v. 1, p. 195–201.

Tankard, A.J., 1986, Depositional response to foreland deformation in the Carboniferous of eastern Kentucky: American Association of Petroleum Geologists Bulletin, v. 70, p. 853–868.

Tetra Tech, Inc., 1981b, Evaluation of Devonian shale potential in Ohio: U.S. Department of Energy, Morgantown Energy Technology Center, Report DOE/METC-122, 61 p.

Thomas, W.A., 1985, The Appalachian-Ouachita connection: Paleozoic orogenic belt at the southern margin of North America: Ann. Rev. Earth Planet, v. 13, p. 175–199.

Timonin, N.I., Yudin, V.V., Belyaev, A.A., 2004, The paleogeodynamics of Pay-Khoy (In Russian): Ekaterinburg, UrD RAS, 229 p.

Tollo, R.P., Bartholomew, M.J., Hibbard, J.P., and Karabinos, P.M., 2010, From Rodinia to Pangea: The Lithotectonic record of the Appalachian region: Geological Society of America Memoir 206, 956 p.

Toro, J., Miller, E.L., Prokopiev, A.V., Zhang, X., and Veselovskiy, R., 2016, Mesozoic orogens of the Arctic from Novaya Zemlya to Alaska: Journal of the Geological Society, v. 173, p. 989–1006.

Torsvik, T.H., and Cocks, L.R.M., 2017, Earth history and palaeogeography: Cambridge, Cambridge University Press, 324 p.

Tugarova, M., Pchelina, T., Ustinov, N., and Viskunova, K., 2008, Lithological and geochemical characteristics of Triassic sediments from the central part of the South Barents depression (Arkticheskaya-1 well): Polar Research, v. 27, p. 495–501.

Uchman, A., Hanken, N.-M., Nielsen, J. K., Grundvåg, S.-A., and Piasecki, S., 2016, Depositional environment, ichnological features and oxygenation of Permian to earliest Triassic marine sediments in central Spitsbergen, Svalbard: Polar Research, v. 35, p. 1–21.

Ulmishek, G., 1986, Stratigraphic aspects of petroleum resource assessment, in Rice, D. D., eds., Oil and Gas Assessment: Methods and Applications, United States of America: American Association of Petroleum Geologists, p. 59–68.

Ulmishek, G.F, and Klemme, H. D., 1990, Depositional controls, distribution, and effectiveness of world's petroleum source rocks: U.S. Geological Survey Bulletin, v. 1931, p. 1–59.

Ustritskiy, V.I., and Tugarova, M.A., 2013, Barents Sea – Permian and Triassic reference section, encountered by the well Admiralteyskaya-1 (in Russian): Neftegasovaâ Geologiâ, Teoriâ i Practika, 8, p. 1–20.

Viele, G.W., 1989, The Ouachita orogenic belt, *in* Hatcher, R.D., Jr., Thomas, W.A., and Viele, G.W., eds., The Appalachian-Ouachita Orogen in the United States, The Geology of North America: Boulder, Geological Society of America, v. F-2, p. 555–561.

Volkov, S.N., 1963, On the question of the relationship of the Urals, Pai-Khoy and Taimyr: VSEGEI, v. 92, p. 25–27.

Vyssotski, A.V., Vyssotski, V.N., and Nezhdanov, A.A., 2012, Evolution of the West Siberian basin, *in* Roberts, D.G., and Bally, A.W., eds., Regional Geology and Tectonics: Phanerozoic Passive Margins, Cratonic Basins and Global Tectonic Maps: Amsterdam, Elsevier, v. 1, p. 755–801.

Walcott, R.I., 1970, Isostatic response to loading of the crust in Canada: Canadian Journal of Earth Sciences, v. 7, p. 2–13.

Wilson, J.T., 1966, Did the Atlantic close and then re-open?: Nature, v. 211, p. 676–681.

Worsley, D., 2008, The post-Caledonian development of Svalbard and the western Barents Sea: Polar Research, v. 27, p. 298–317.

Xie, X., and Heller, P.L., 2009, Plate tectonics and basin subsidence history: Geological Society of America Bulletin, v. 121, p. 55–64.

Zhang, X., Pease, V., Carter, A., and Scott, R., 2018, Reconstructing Palaeozoic and Mesozoic tectonic evolution of Novaya Zemlya: combining geochronology and thermochronology, *in* Pease, V., and Coakley, B., eds., Circum-Arctic Lithosphere Evolution: London, The Geological Society, Special Publications, v. 460, p. 335–353.

Zhuravlev, V.A., Korago, E.A., Kostin, D.A., and Zuikova, O.N., 2014, State geological map of the Russian Federation (in Russian): Saint Petersburg, VSEGUEI, The North-Kara-Barents Sea Series, Sheets R-39 and R40, Scale 1: 1,000,000.

Ziegler, P.A., 1989, Evolution of Laurussia: Dordrecht, Kluwer Academic Publishers, 102 p.

Table 1: Schematic comparison between the Appalachian and BSS areas in terms of general features, tectonics, stratigraphy, and paleogeography. Please refer to text for detailed description and discussions.

Items	Appalachian area	Barents Sea shelf area
Approximate area (km^2)	0.93 million (Appalachian foreland and intracratonic areas)	1.4 million (shelf area)
Present-day setting	Continental	Mostly Offshore
Approximate maximum thickness (km)	13.7 (Appalachian Basin); 6.0 (Illinois Basin); and 4.3 (Michigan Basin)	Unknown. More than 20 km is believed in the South Barents Basin. At least 10 km in western basins.
Exploration status	Mature	Mostly frontier
Tectonics		
Structural elements (present day)	Foreland and intracratonic basins; structural highs and platforms. Nine superimposed foreland basins	Foreland, intracratonic, rift and strike-slip basins. Structural highs and platforms. Abundance of structural highs
Diachronous collisional events associated with oceanic closure	Closure of Iapetus and Rheic Oceans	Closure of Iapetus and Uralian Oceans
Stratigraphy		
Overall succession	Clastic-carbonate-clastic	Clastic-carbonate-clastic
Foreland basin succession	Easily identified. Several superimposed foreland basins.	Not easily identified. At least one Mesozoic and one Paleozoic basin

Unconformities	Multiple. Local and regional	Multiple. Local and regional
Level of foreland preservation	Very good. Most foreland lithologies are preserved regionally	Variable. The Paleozoic foreland basin(s) were structurally inverted by thrusting and destroyed by erosion
Carbonate platforms	Warm water (stable platform, abundant); salt is not abundant; cold water (following the beginning of collision); chert is present at local to basinal scale	Warm water (stable platform, abundant); salt is common to abundant; cold water (following the beginning of collision); chert is present at a regional scale
Paleogeography		
Overall paleoclimate succession	Humid-arid-humid	Humid-arid-humid
Paleocontinent development in time	Laurentia-Laurussia-central Pangea	Baltica-Laurussia-northern Pangea
Influence of major glaciation	Ordovician, Devonian, and Permo-Carboniferous	Permo-Carboniferous and Late Cenozoic

Table 2: General comparison between the Appalachian and BSS areas in terms of timing and tectonic events.

Stages		Appalachian area		Barents Sea shelf area	
		Timing	Event	Timing	Event
1.	Basement precursors	Precambrian	Presence of Precambrian basement structures	Late Precambrian–Late Devonian	Presence of Timanian and Caledonian basement structures
2.	Orogenic collapse and relaxation	Late Precambrian–early Cambrian	Relaxation, rifting, erosion, and deposition of continental clastics	Late Devonian–Early Carboniferous	Caledonian relaxation, rifting, erosion, and deposition of continental clastics (western BSS)
3.	Stable platform development	Middle Cambrian–Early Ordovician	Stable platform development	Late Carboniferous–Early Permian	Stable platform development (behind offshore arc to the east)
4.	Inception of subduction-type orogeny (s) with bulge migration and foreland-basin development	Early–Middle Ordovician	Inception of Taconian Orogeny with unconformity and initiation of basal tectophase	Early Permian	Pennsylvanian inception of orogeny with unconformity and initiation of basal tectophase
5.	Deformational loading and platform subsidence to develop a foreland	Middle Ordovician–Mississippian	Deformational loading and platform subsidence	Permian–earliest Triassic (at least one	Deformational loading and platform subsidence (cherty

	basin (one or more tectophases)	(during four orogenies and nine tectophases)	(marine black shales during each of nine tectophases)	tectophase during one orogeny)	limestones to black shales)
6.	Relaxation through infilling of foreland basin with syn- and post-orogenic clastics; termination of tectophase (one or more tectophases)	Late Ordovician–Mississippian (during four orogenies and nine tectophases)	Infilling of foreland and some intracratonic basins with syn- and post-orogenic clastics (flysch- and molasse-like clastics during each of nine tectophases)	Permian–Late Triassic	Infilling of foreland and some intracratonic basins with syn- and post-orogenic clastics (flysch- and molasse-like clastics during at least one tectophase)
7.	Final ocean closure and continental collision with major unconformity development, overlain by a largely terrestrial clastic wedge	Pennsylvanian–Permian	Mississippian-Pennsylvanian unconformity, overlain by a largely terrestrial clastic wedge, migrating far beyond the foreland basin	Lower–Middle Jurassic	Triassic-Jurassic unconformity, overlain by a largely terrestrial clastic wedge, migrating far beyond the foreland basin
8.	Beginning of Atlantic cycle	Late Triassic–Jurassic	Orogenic collapse, rift development and infill	Late Jurassic–Eocene	Transpression on western part of BSS and oceanic flooding

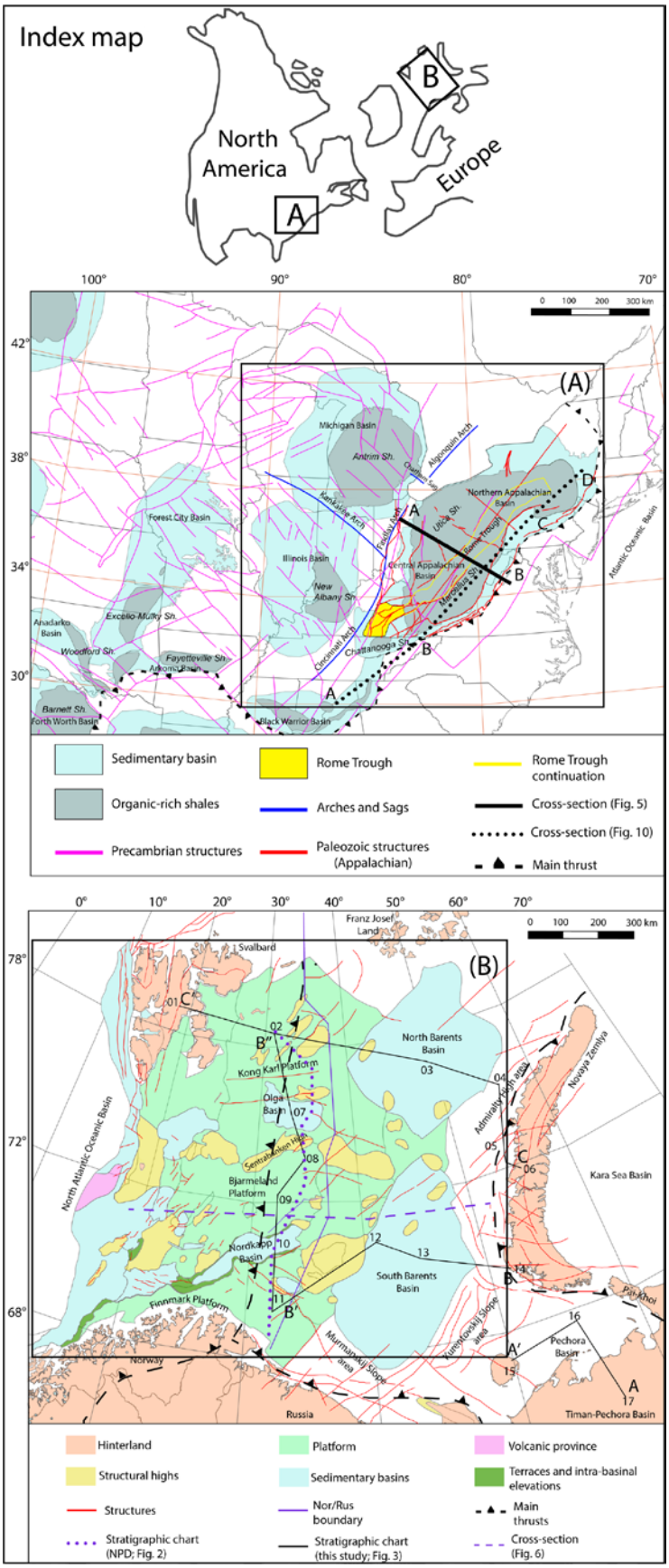
Index map
North America
Europe
A
B
100°
90°
80°
70°
42°
38°
34°
30°
0 100 200 300 km
(A)
Michigan Basin
Antrim Sh.
Algonquin Arch
Kankakee Arch
Forest City Basin
Illinois Basin
New Albany Sh.
Cincinnati Arch
Chattanooga Sh.
Ohio Sh.
Rome Trough
Northern Appalachian Basin
Central Appalachian Basin
Marcellus Sh.
Atlantic Oceanic Basin
Anadarko Basin
Excello-Mulky Sh.
Woodford Sh.
Fayetteville Sh.
Arkoma Basin
Barnett Sh.
Forth Worth Basin
Black Warrior Basin
Sedimentary basin
Organic-rich shales
Precambrian structures
Rome Trough
Arches and Sags
Paleozoic structures (Appalachian)
Rome Trough continuation
Cross-section (Fig. 5)
Cross-section (Fig. 10)
Main thrust
0°
10°
20°
30°
40°
50°
60°
70°
78°
72°
68°
0 100 200 300 km
(B)
Franz Josef Land
Svalbard
North Barents Basin
Kong Karl Platform
Olga Basin
Admiralty Arch
Novaya Zemlya
North Atlantic Oceanic Basin
Bjarmeland Platform
Kara Sea Basin
Nordkapp Basin
South Barents Basin
Finnmark Platform
Pay-Khoi
Murmanskij Slope area
Norway
Russia
Pechora Basin
Timan-Pechora Basin
Hinterland
Structural highs
Structures
Stratigraphic chart (NPD; Fig. 2)
Platform
Sedimentary basins
Nor/Rus boundary
Stratigraphic chart (this study; Fig. 3)
Volcanic province
Terraces and intra-basinal elevations
Main thrusts
Cross-section (Fig. 6)

Fig. 1: Map A) Main structural elements and major shale-play systems in the eastern, central, and northern United States. The Appalachian foreland and adjacent intracratonic basins are included in the black rectangle. The Ouachita system of basins and platforms is partially represented in the southern and southwestern parts of the figure. The Rome Trough (yellow) represents a pre-Appalachian system of rift basins. The solid and dotted black lines represent section lines in Figures 5 and 10, respectively. The former Appalachian Mountains are represented by an area of complexly deformed and metamorphosed rocks to the east of the Appalachian Basin. Data were compiled from the Energy Information and Administration EIA (2021, sedimentary basins and organic-rich plays); Tetra Tech (1981, arches and sags); Repetski et al. (2008, Paleozoic structures); and Sims et al. (2008, Precambrian structures). Map B) Main structural elements of the Barents Sea shelf (BSS) region. The red lines illustrate a highly schematic structural lineament framework (NPD, 2021). The solid purple line is the offshore boundary (NPD, 2017) between the Norwegian (western) and Russian (eastern) BSS sectors. The dotted and dashed purple lines are stratigraphic section lines in Figures 2 and 6, respectively. The solid black lines are stratigraphic section lines in Figure 3. The black-dashed lines represent Caledonian, Timanian, and Uralian-Pai-Khoi-Novaya Zemlya thrust fronts (Drachev, 2016). The North and South Barents basins represent present-day expression of the Uralide foreland basin on the BSS; the central highs at longitude 38°–40° represent a probable forebulge area; and the structurally complex area on the Norwegian side represents intracratonic basins and intervening platform areas. Structural elements were compiled from the NPD (2021).

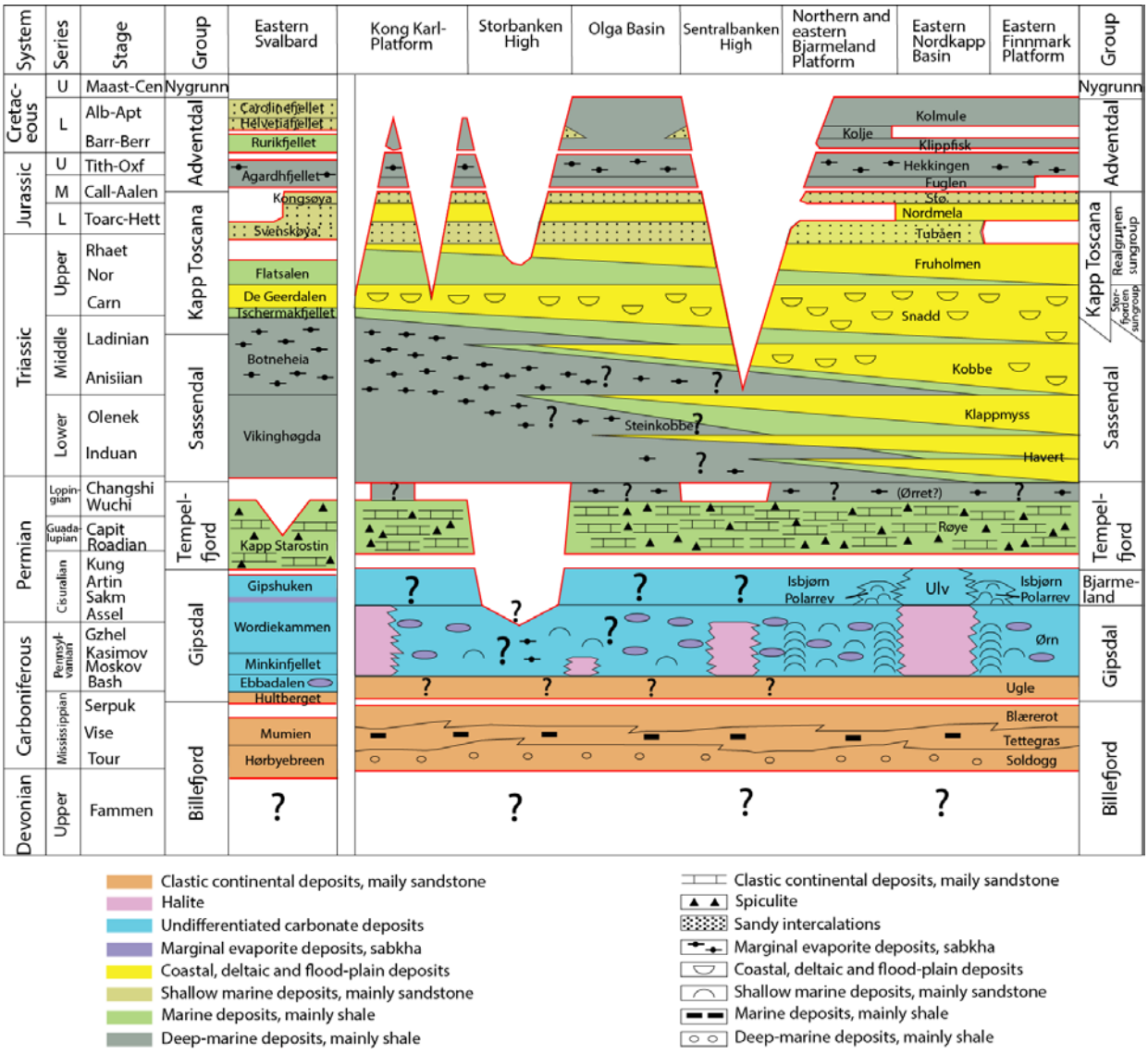

Fig. 2: Schematic chronostratigraphic and lithostratigraphic diagram for eastern areas of the Norwegian BSS and a generalized stratigraphic column for eastern Svalbard (left-most column, modified from NPD, 2017) (dotted purple line in Fig. 1B). The question marks represent uncertainties concerning the interpretation of, facies, and source-rock occurrence. Comparison with Figure 3 shows that this figure is a very generalized regional stratigraphic interpretation, which also lacks stratigraphy from the eastern BSS.

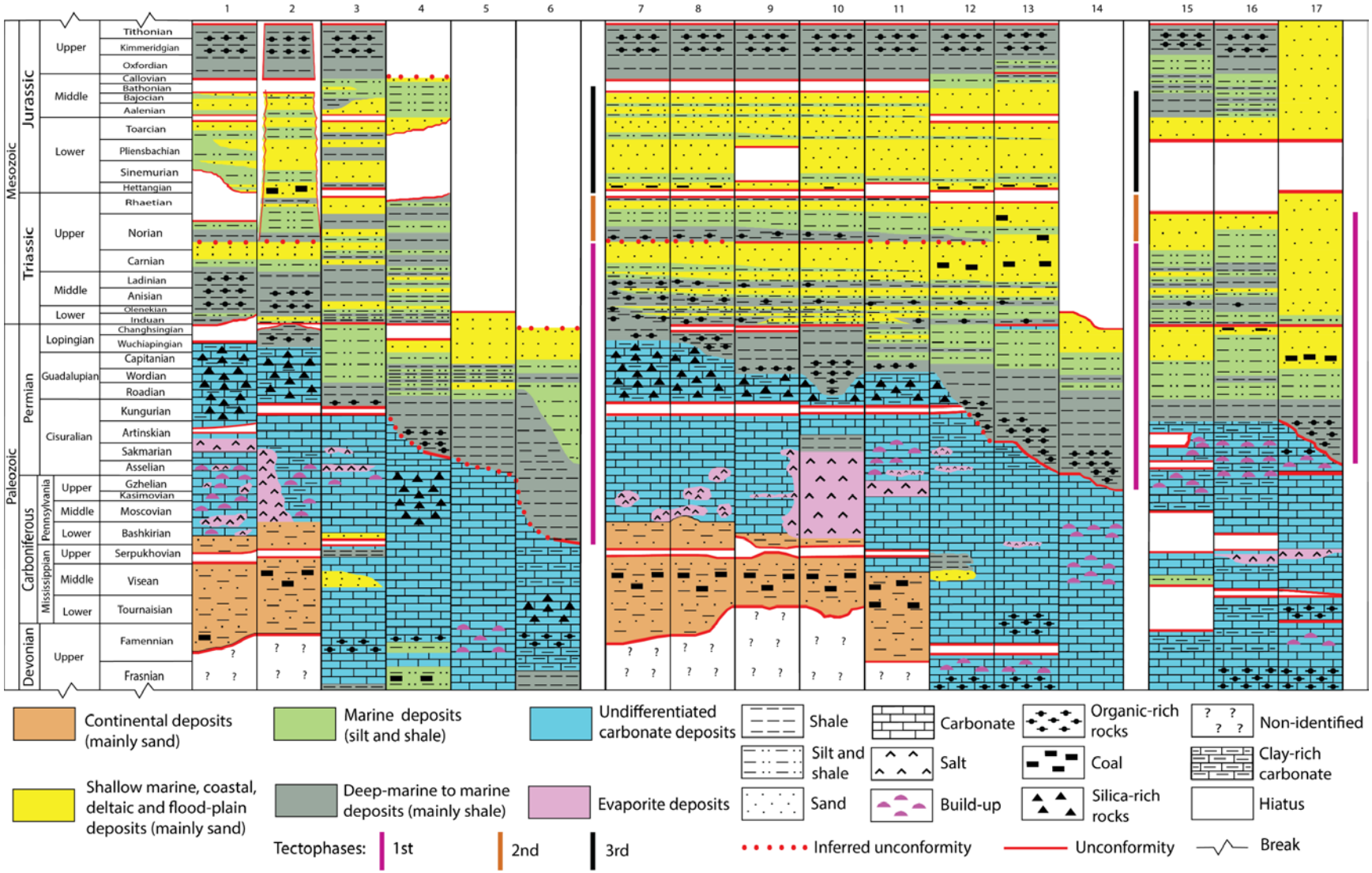
1
2
3
4
5
6
7
8
9
10
11
12
13
14
15
16
17
Mesozoic
Paleozoic
Jurassic
Triassic
Permian
Carboniferous
Devonian
Pennsylvania
Mississippian
Upper
Middle
Lower
Tithonian
Kimmeridgian
Oxfordian
Callovian
Bathonian
Bajocian
Aalenian
Toarcian
Pliensbachian
Sinemurian
Hettangian
Rhaetian
Norian
Carnian
Ladinian
Anisian
Olenekian
Induan
Changhsingian
Wuchiapingian
Capitanian
Wordian
Roadian
Kungurian
Artinskian
Sakmarian
Asselian
Gzhelian
Kasimovian
Moscovian
Bashkirian
Serpukhovian
Visean
Tournaisian
Famennian
Frasnian
Lopingian
Guadalupian
Cisuralian
Continental deposits (mainly sand)
Shallow marine, coastal, deltaic and flood-plain deposits (mainly sand)
Marine deposits (silt and shale)
Deep-marine to marine deposits (mainly shale)
Undifferentiated carbonate deposits
Evaporite deposits
Shale
Silt and shale
Sand
Carbonate
Salt
Build-up
Organic-rich rocks
Coal
Silica-rich rocks
Non-identified
Clay-rich carbonate
Hiatus
Tectophases:
1st
2nd
3rd
Inferred unconformity
Unconformity
Break

Fig. 3: Schematic tectonostratigraphic section (solid black line in Fig. 1B) of eastern Spitsbergen (1); BSS (2–4; 7–13); Novaya Zemlya (5; 6; 14); Pechora Basin (15; 16) and northeastern Timan-Pechora Basin (17). The time scale reflects the International Chronostratigraphic Chart (Cohen et al., 2013). Colors represent generic depositional environments. Colored lines on the right-hand margins of each section represent tectophases in the main Uralian (purple) and Novaya Zemlya (orange and black) orogenies. Key references, but not the only references, used in constructing the section include: Timan-Pechora Basin (e.g., Abrams et al., 1999; Prischepa et al., 2011; Schenk, 2011); Pechora Basin (e.g., Ivanova, 1997; Suvorova and Matveeva, 2014; Norina et al., 2014; Zhuravlev et al., 2014); Novaya Zemlya (e.g., Nakrem, 2007; Drachev, 2016; Zhang et al., 2018); BSS (e.g., Dalland et al., 1988; Johansen et al., 1993; Grogan et al., 1999; Larssen et al., 2002; Margulis, 2008, Leonchik and Senin, 2010; Tugarova et al., 2008; Smelror et al., 2009; Henriksen et al., 2011; Stoupakova et al., 2011; Ustritskiy and Tugarova, 2013; Polyakova, 2015; Burguto et al., 2016; NPD, 2017; Olaussen et al., 2018); eastern Spitsbergen (e.g., Stemmerik and Worsley, 2005; Riis et al., 2008; Dallmann et al., 2015; Nicolaisen et al., 2019).

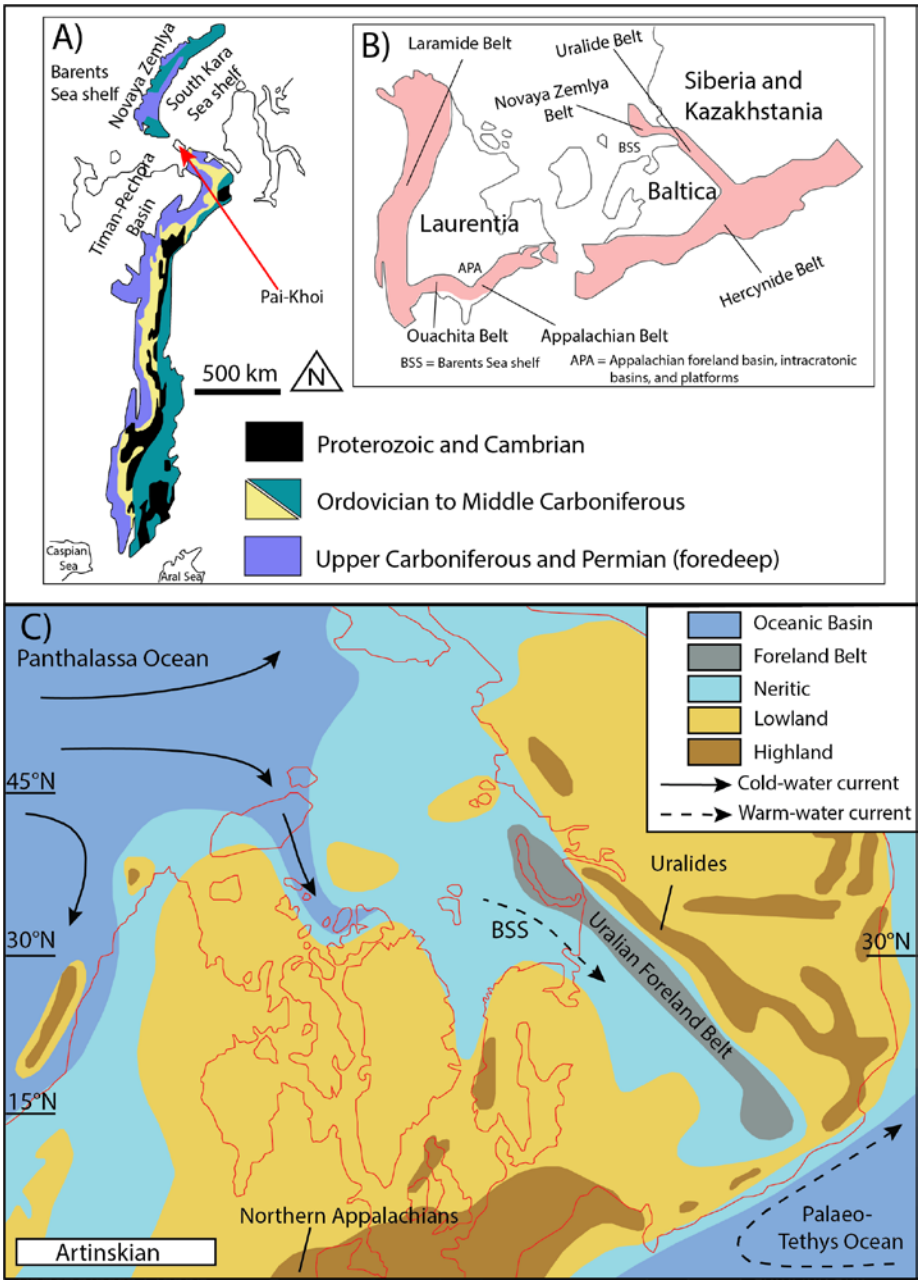

Fig. 4: A) Extent of the Uralide fold belt and associated facies; Ordovician to Middle Carboniferous deposits are pre-orogenic, mostly platform, sequences. Although not highlighted in the figure, Proterozoic rocks are locally exposed on Novaya Zemlya (e.g., Evdomikov et al., 2000). B) Major Hercynian-aged fold belts involved in the final amalgamation of Pangea (modified from Proust et al., 1998). C) Paleogeographic reconstruction illustrating the convergence of Laurussia (southeastern continent) and Siberia-Kazakhstania (northeastern continent) during Artinskian time, and the location of the Uralides and adjacent foreland basin belt, which includes the area that is now the Novaya Zemlya archipelago (northwestern-most area of the belt). The distribution of warm and cold

currents reflects results related to closure of the sea-way connection between the Uralides and the Paleo-Tethys Ocean (modified from Reid et al., 2007).

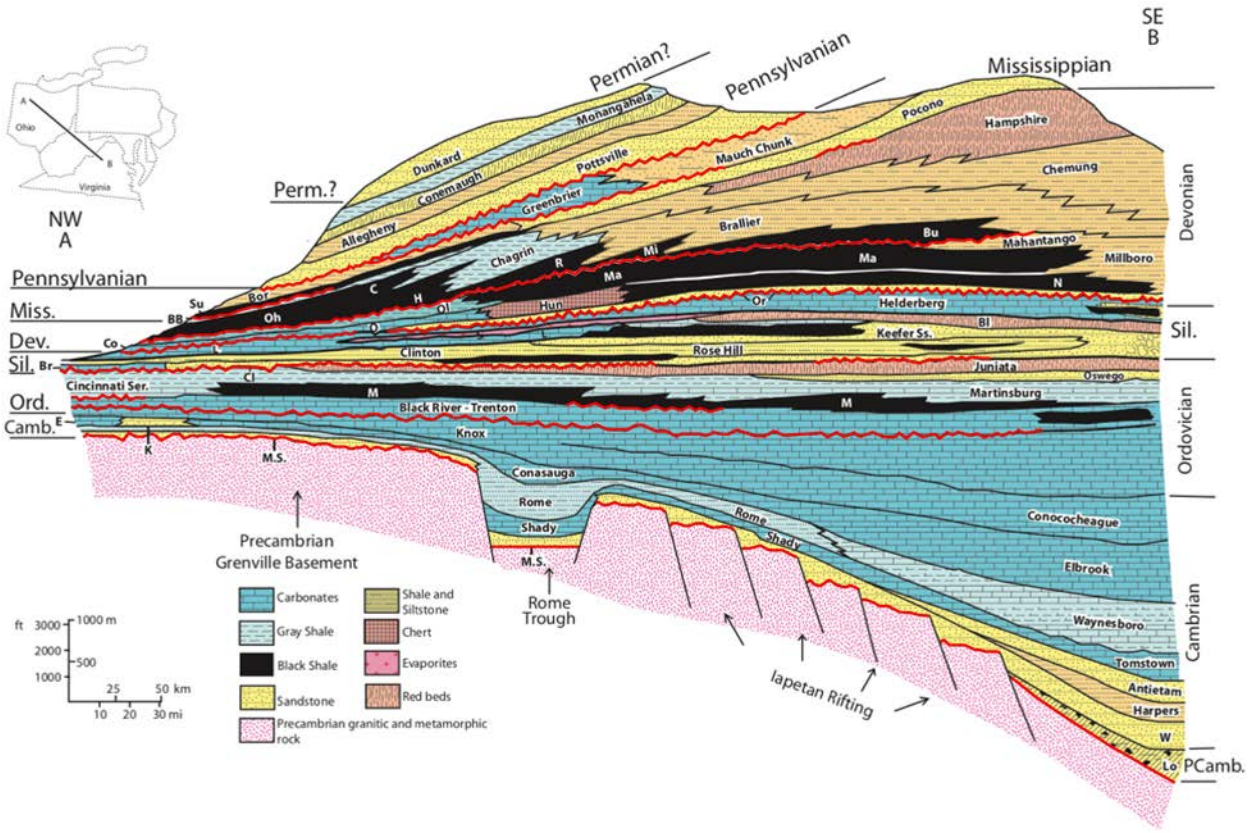

Fig. 5: Schematic northwest-southeast cross section across the north-central Appalachian foreland basin, illustrating major stratigraphic relationships and stratigraphic units (Fig. 1A; solid black line). The Mid-Ordovician unconformity represents inception of the U.S. Appalachian foreland basin. The unconformity-bound stratigraphic units reflect the following orogenies: Ordovician (Taconian); Silurian (Salinic); Devonian (Acadian); Mississippian (Neoacadian) and Pennsylvanian–Permian (Alleghanian). Note the presence of Precambrian basement structures, related to earlier pre-Appalachian rifting, which were periodically reactivated during later Appalachian orogenies. Lo=Loudon Fm.; W=Weverton Ss.; MS=Mt. Simon Ss.; K=Kerbel Fm.; E=Eau Claire Fm.; M=Martinsburg Sh.; Br=Brassfield Lms.; T=Tuscarora Ss.; L=Lockport Dol.; Bl=Bloomsburg Fm.; S=Salina Gr.; Co=Columbus Lms.; O=Onondaga Lms.; Hun=Huntersville Chert; Or=Oriskany Ss.; N=Needmore Sh.; Ma=Marcellus Sh.; Bu=Burket Sh.; Mi=Middlesex Sh.; R=Rhinestreet Sh.; H=Huron Sh.; C=Cleveland Sh.; Oh=Ohio Sh.; Ol=Olentangy Sh.; BB=Bedford-Berea; Su=Sunbury Sh.; Bor=Borden Fm. (modified from Ettensohn et al., 2019).

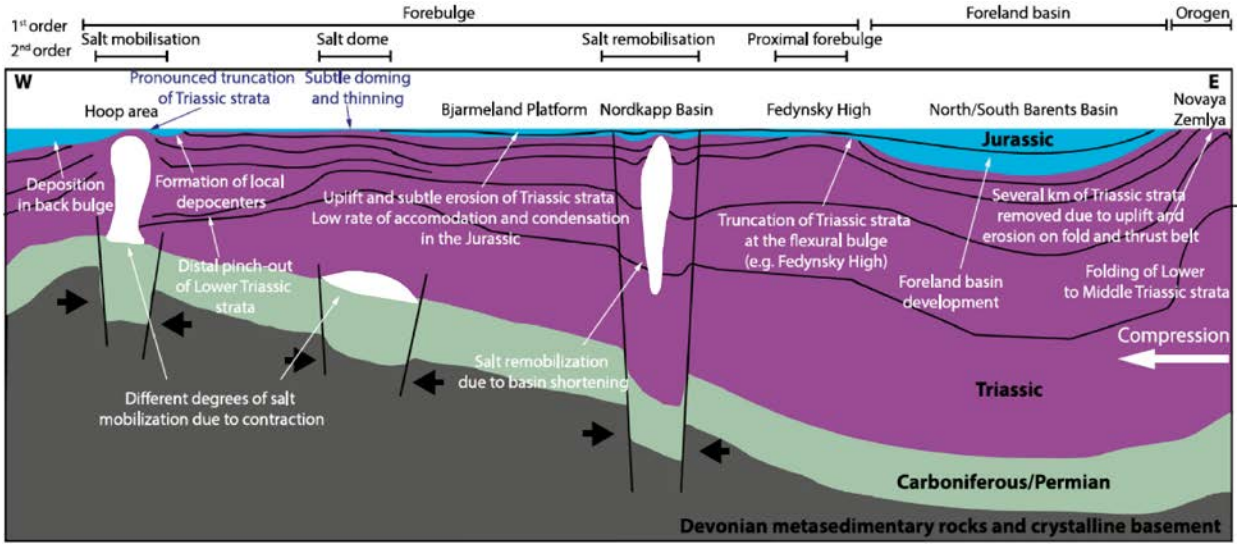

Fig. 6: Cross section (Fig. 1B; dashed purple line) showing the interpreted Devonian–Jurassic succession in the BSS, as well as major structural elements, structural reactivation, and salt mobilization due to westward compression from the Novaya Zemlya Orogeny (modified from Müller et al., 2019).

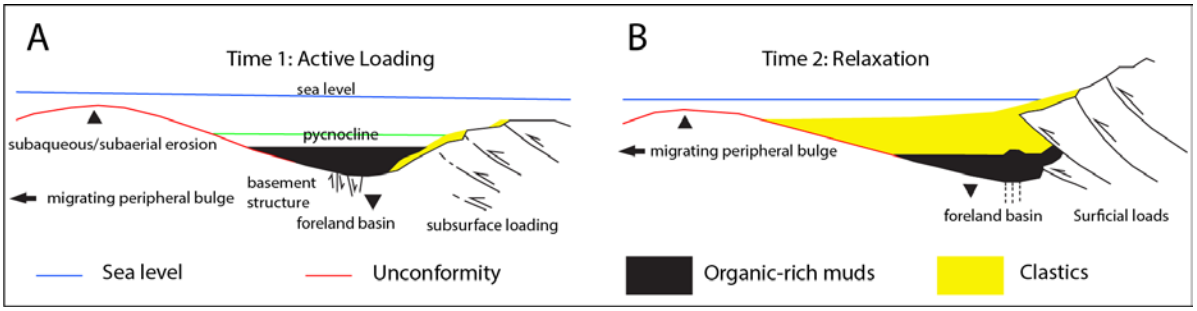

Fig. 7: Sequential schematic diagrams showing flexural relationships among foreland-basin formation, sediment infill and deformational loading. A) Basin-bulge formation and migration with subaqueous deformational loading and little clastic influx (represents first three parts of the tectophase cycle; Fig.8B). Major surficial deformational loading with major clastic influx during part 4 of the tectophase cycle. The pycnocline is a zone of thermohaline density stratification lacking O_2 below which organic-rich muds can be preserved (▲= peripheral bulge; ▼= axis of foreland basin; modified from Ettensohn et al., 2019).

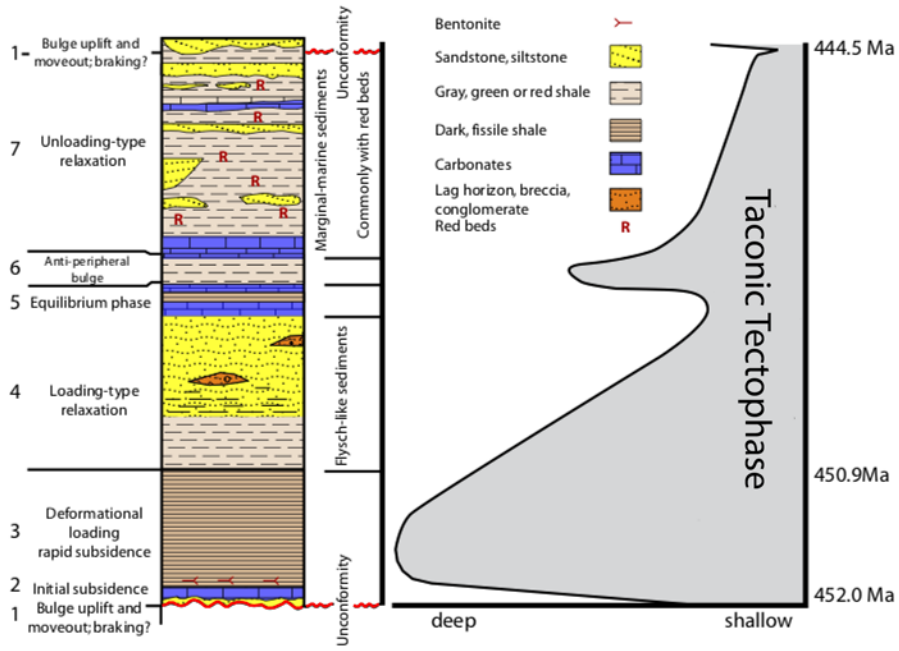

Fig. 8: Schematic lithologic succession representing a generalized tectophase cycle at the outcrop scale with a eustatic curve for early subduction-type orogenies using the Appalachian, Taconic tectophase and ages as an example. The sequences are typically unconformity-bound but may be incomplete or eroded (modified from Ettensohn, 1994, and Ettensohn et al., 2019).

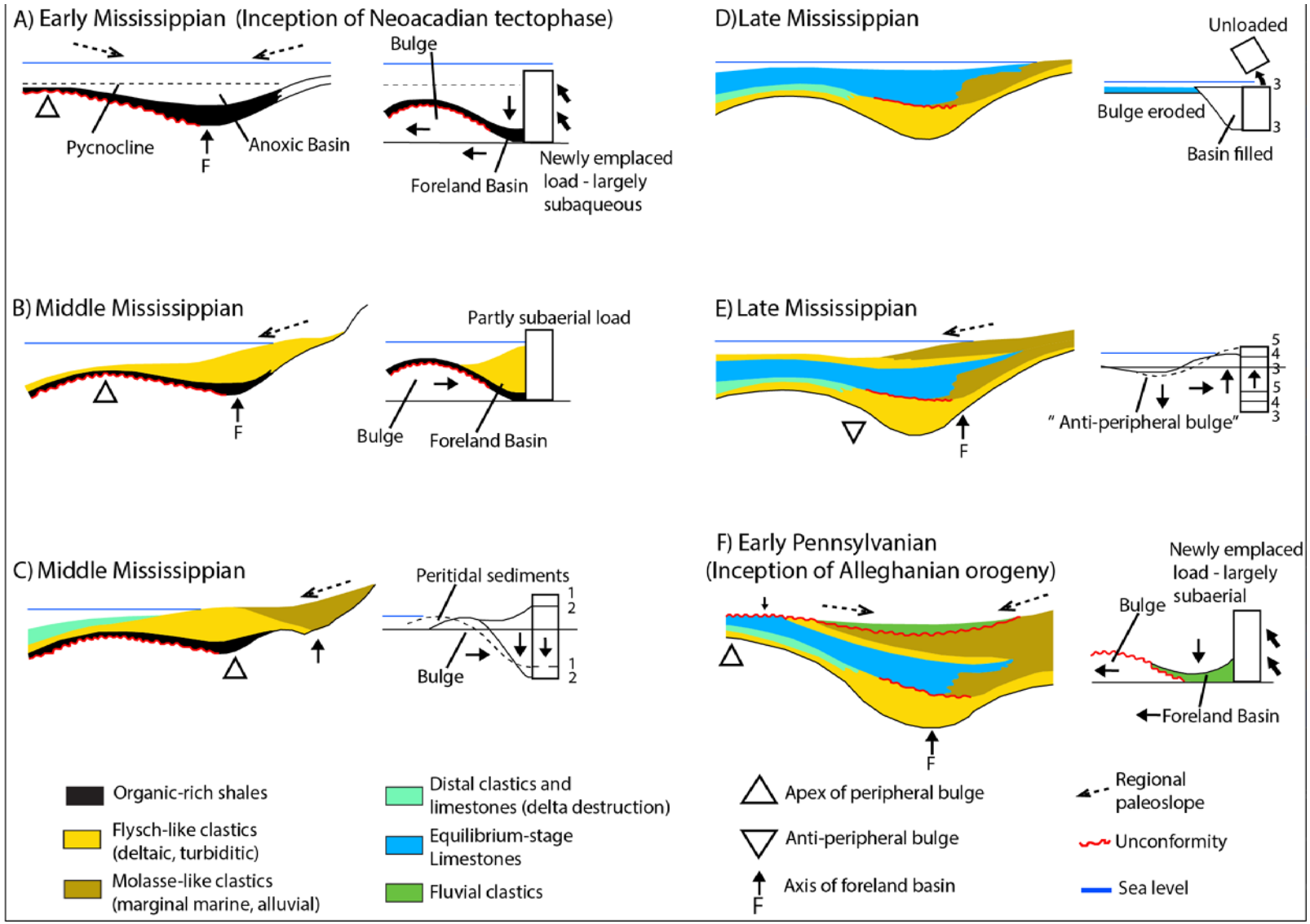

Fig. 9: Complete Mississippian Neoacadian tectophase sequence from the Appalachian Basin showing the stage in the tectophase model to the right and the accompanying stratigraphic response to the left. A) Same as Figures 7A

and 8, parts 1[lower unconformity], 2, 3). B) and C) Same as Figure 7B and Figure 8, part 4. D) Same as Figure 8, part 5. E) Same as Figure 8, parts 6, 7F) Figure 8, part 1, upper unconformity and new Alleghanian tectophase (modified from Ettensohn et al., 2012).

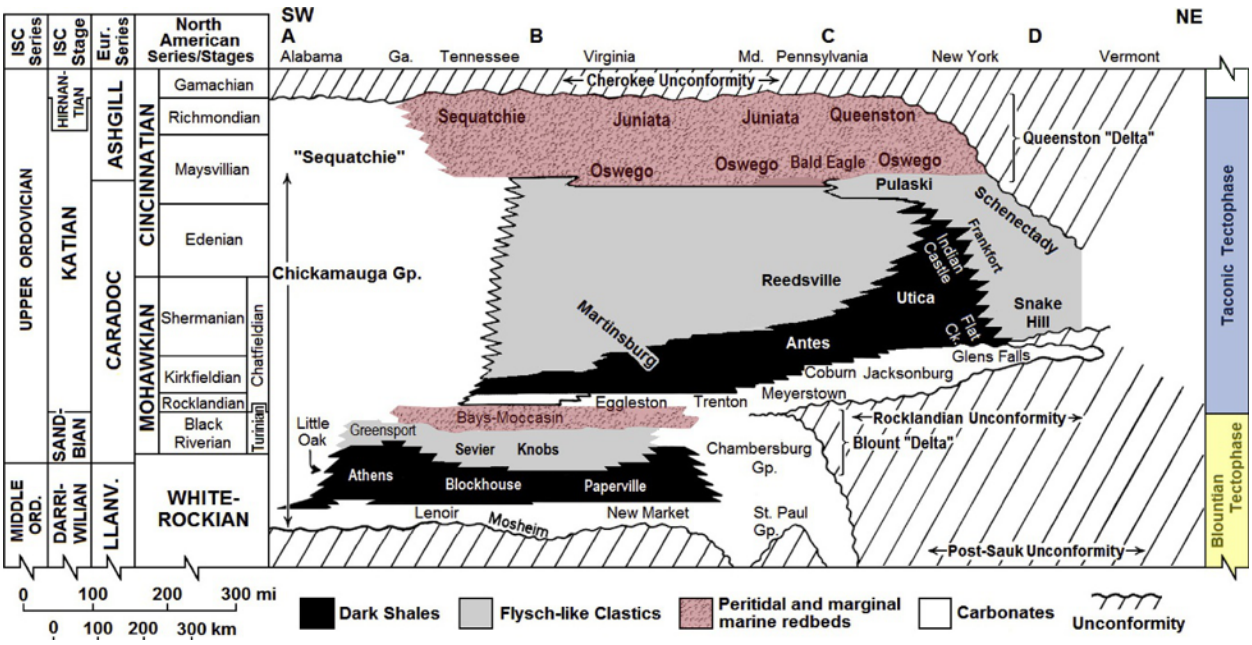

Fig. 10: Schematic, southwest-northeast, Middle–Upper Ordovician section (section ABCD in Fig. 1A) paralleling the strike of the Appalachian Basin and showing repetition of foreland-basin tectophase cycles for the Taconian tectophases, which are marked by a succession consisting of a basal unconformity, thin transgressive carbonate, black-shales, flysch-like sediments, and molasse-like sediments. The younging of the Antes-Utica shales reflects the northward migration in space and time. Ga. = Georgia; Md. = Maryland. No vertical scale intended. (Modified from Ettensohn et al., 2019).

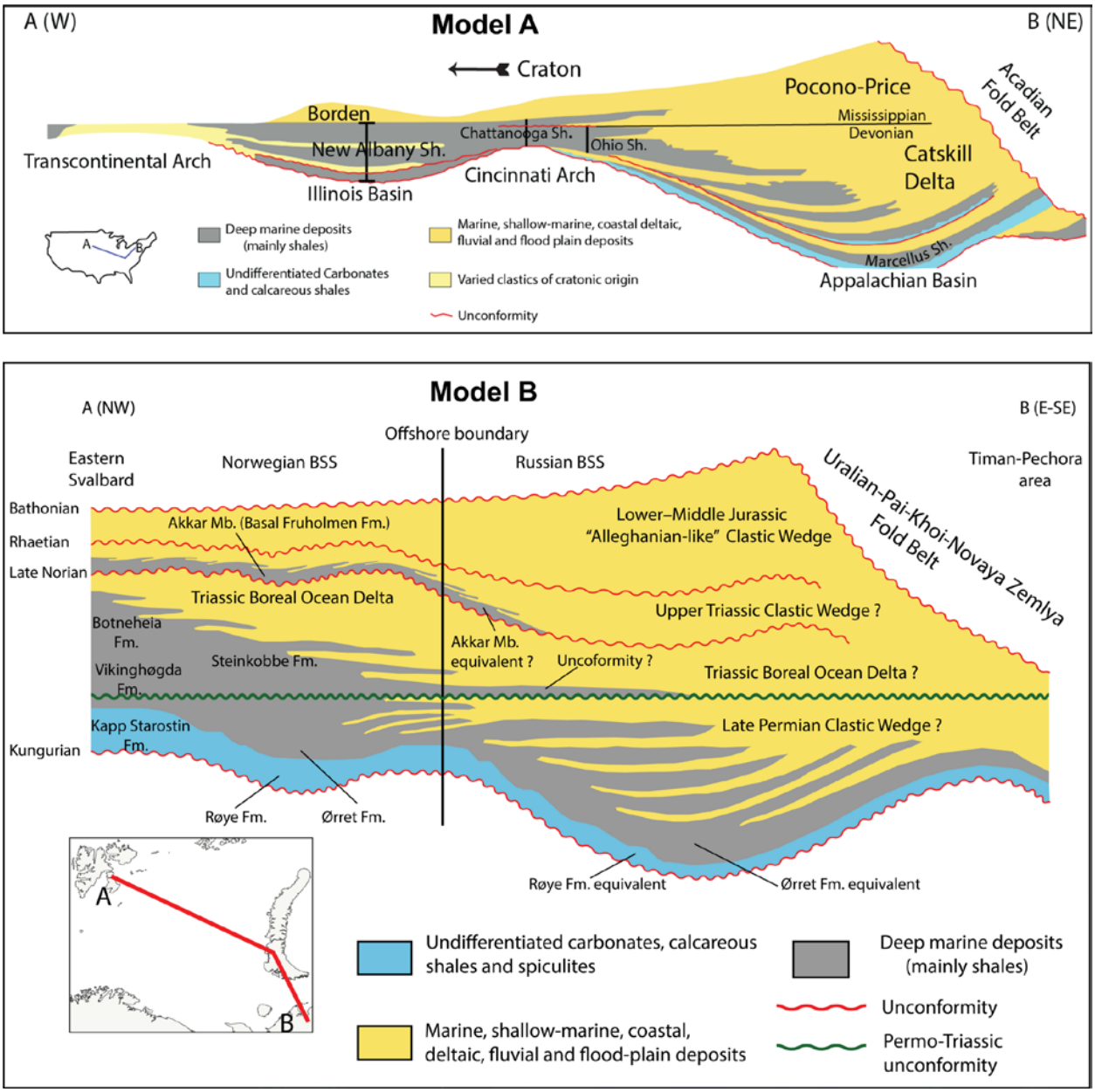

Fig. 11: Model A) shows a highly schematic cross-section, illustrating Devonian–Mississippian black shales in east-central United States and basin yoking during black-shale deposition. Datum is the Devonian-Mississippian boundary, which is a subtle unconformity in parts of the Appalachian Basin. Note the distribution of black shales and coarser clastics, overflowing from the Appalachian foreland basin into the Illinois intracratonic basin (modified from Ettensohn, 1992). Many of these black shales are source rocks for clastic reservoirs throughout the basin. Model B) shows a highly schematic cross-section, illustrating the Late Permian–Middle Jurassic tectonostratigraphic succession in the BSS area, illustrated using an Appalachian-type tectonostratigraphic model (Figs. 8–11A). Datum

is the Permo-Triassic unconformity (green) that represents regional uplift accompanying the Permo-Triassic plume event. Deep marine deposits include organic-rich shales. The unconformities in red are associated with Uralian-Pai-Khoi-Novaya Zemlya tectophases.